# A new digital Lithological Map of Italy at 1:100.000 scale for geo-mechanical modelling

Francesco Bucci[1], Michele Santangelo[1], Lorenzo Fongo[2], Massimiliano Alvioli[1], Mauro Cardinali[1], Laura Melelli[2], Ivan Marchesini[1],

[1] Consiglio Nazionale delle Ricerche, Istituto di Ricerca per la Protezione Idrogeologica, via Madonna Alta 126, I-06128 Perugia, Italy
[2] Università degli Studi di Perugia, Dipartimento di Fisica e Geologia, Piazza dell'Università 1, I-06123 Perugia, Italy
*Correspondence to*: Michele Santangelo (michele.santangelo@irpi.cnr.it)

**Abstract.** Lithological maps contain information about the different lithotypes cropping out in an area. At variance with geological maps, portraying geologic formations, lithological maps may differ as a function of their purpose. Here, we describe the preparation of a lithological map of Italy at the 1:100,000 scale, obtained from classification of a comprehensive digital database and aimed at describing geo-mechanical properties. We first obtained the full database, containing about 300,000 geo-referenced polygons, from the Italian geological survey. We grouped polygons according to a lithological classification by expert analysis of the original 5,456 unique descriptions of polygons, following compositional and geo-mechanical criteria. The procedure resulted in a lithological map with a legend including 19 classes, and it is linked to a database allowing ready interpretation of the classes in geo-mechanical properties, and amenable to further improvement. The map is mainly intended for statistical and physically based modelling of slope stability assessment, geo-morphological and geo-hydrological modelling. Other possible applications include geo-environmental studies, evaluation of river chemical composition, estimation of raw material resources. The dataset is publicly available at https://doi.org/10.1594/PANGAEA.935673 (Bucci et al. 2022).

## 1 Introduction

Lithology encodes information on the composition and physical properties of rocks and, therefore, it is a key variable in the study of earth surface and subsurface processes. As such, lithological analysis is relevant to a large body of literature, including landscape evolution (Coulthard, 2001), water flow paths (Gleeson et al., 2011), landslides (Alvioli et al., 2021; Sarro et al., 2020; Reichenbach et al., 2018), chemical composition of rivers or atmospheric $CO_2$ consumption (Donnini et al 2020; Hartmann et al., 2010; Gibbs, 1994), soil classification (de Sousa et al., 2020), soil erosion (Vanmaercke et al., 2021), seismic amplification (Mori et al., 2020; Forte et al., 2019), groundwater level variability (de Graaf et al., 2017; Lorenzo-Lacruz et al., 2017), floods (Vojtek & Vojteková, 2019), oil reservoirs (Han et al., 2018), geothermal potential (Roche et al., 2019), geomorphological classification (Alvioli et al., 2020) and many others. Lithological variability is often a measure of geological and landscape complexity, and provides important information on geological evolution and heritage (Bucci et al., 2019; Ispra & Parco Nazionale del Cilento, Vallo di Diano e Alburni, 2013, Santangelo et al., 2013), geo-resources settings (Bucci et al., 2016a; Ge.Mi.Na., 1962; Corpo Reale delle Miniere 1926-1935) geo-environmental risks (Giustini et al., 2019; Bentivenga et al., 2004) and matter fluxes at the Earth's surface (Brogi & Liotta, 2011; Boni et al., 1984).

Lithological heterogeneity should be therefore sufficiently represented in maps at the local, regional and supra-regional scale. Lithological information is commonly derived from geological maps. In recent years, much effort has been made to make the geological data available around the world accessible at the best possible scales (Table 1, ID 1, 2). However, this still remains an open challenge because the quality, scale, updating and availability of geodata varies enormously across the globe.

| ID | Services/products/data | Type | URL | Institutions | Context |
|---|---|---|---|---|---|
| *1* | *Visualization of the Geological map of the world at the best possible scales* | WebMap | http://portal.onegeology.org/OnegeologyGlobal/ | Onegeology | Global |
| *2* | *General geologic map of the world at approximately 1:35,000,000 scale* | WebMap | https://mrdata.usgs.gov/geology/world/map-us.html#home | Geological Survey of Canada | Global |
| *3* | *Geologic Map Databases for the United States* | WMS, WFS, Download vector data | https://mrdata.usgs.gov/geology/state/ | USGS | (Sub-) Continental USA |
| *4* | *Pan-European and national geological datasets and services from the Geological Survey Organizations of Europe* | WMS, WFS, Download vector data | http://www.europe-geology.eu/onshore-geology/geological-map/ | EuroGeoSurvey | (Sub-) Continental Europe |
| *5* | *Geoportal of the Italian Geological Survey (ISPRA)* | WMS, WFS, Download vector data | http://sgi2.isprambiente.it/viewersgi2/ | ISPRA | National Italy |
| *6* | *Visualization of the available (in raster format) geological sheets of Italy at 1:100.000 scale* | Web application | http://sgi.isprambiente.it/geologia100k/ | ISPRA | National Italy |
| *7* | *Visualization of the available (in raster format) geological sheets of Italy at 1:50.000 scale* | Web application | https://www.isprambiente.gov.it/Media/carg/index.html | ISPRA | National Italy |
| *8* | *Guidelines for the realization of the Geological and Geotechnical Map at the scale 1:50.000* | Web Page | https://www.isprambiente.gov.it/en/projects/soil-and-territory/carg-project-geologic-and-geothematic-cartography | ISPRA | National Italy |
| *9* | *REST service provided by ISPRA for the publication of spatial data* | REST | http://sgi2.isprambiente.it/arcgis/rest/services/servizi/carta_geologica_100k/MapServer/ | ISPRA | National Italy |

**Table 1:** Uniform Resource Locators (URL) of the institutional services, guidelines, products or datasets consulted for compiling our map.

The situation is more homogeneous at the continental or sub-continental level. For example, in 2017 the U.S. Geological Survey published a compilation of the individual releases of the Preliminary Integrated Geologic Map Databases (SGMC) for the United States (Table 1, ID 3), which represents a seamless, spatial database of 48 State geologic maps that range from 1:50,000 to 1:1,000,000 scale (Horton, 2017). The SGMC is not a truly integrated geologic map database because geologic units have not been reconciled across State boundaries. However, the geologic data contained in maps for individual States have been standardized to allow spatial analyses of lithology, age, and stratigraphy.

In Europe, in 2016 the EuroGeoSurvey launched the European Geological Data Infrastructure (EGDI, Table 1, ID 4). EGDI provides access to Pan-European and national geological datasets and services from the Geological Survey Organizations of Europe. Geological Layers available include the Geological map of Europe, 1:5,000,000 scale, and the surface lithology of Europe, 1:1,000,000 scale. More detailed geologic or geological derived maps are available at national scale only (Table 1, ID 5, 6).

In Italy, the existing geological maps with national coverage (Console et al., 2017) are at 1:1,250,000 (Bonomo et al., 2005) 1:1,000,000 (Pantaloni, 2011; Cipolloni et al., 2009; Compagnoni, 2004), 1:500,000 (Compagnoni et al., 1976-1983), and 1:100,000 scale (Servizio Geologico d'Italia, 2004) and are managed by ISPRA (Istituto Superiore per la Protezione e la Ricerca Ambientale - De Logu et al., 2012). The 1: 50,000 national geological map, coordinated and published by ISPRA, has an incomplete coverage of the Italian territory (Table 1, ID 7, 8).

Some of the above mentioned maps are accessible, for display purposes only, via standard view services (WMS -Web Map Service, Table 1, ID 5).

Amanti et al., (2007) and (2008), described the first known attempt by ISPRA to draft a lithological map of Italy at the 1:100,000 scale. The published map covers the 65% of the national territory and does not include Sardinia, Sicily and the sheets 156 to 176, 183 to 187 and 196 to 199. This lithological map is not accessible in raster or vector format.

In 2018, ISPRA completed the work published in the 2007 and 2008 publications, and a lithological cartography of the entire Italian territory at 1:100,000 scale, was made accessible for visualization, through the geo-portal (Table 1, ID 5). The map was obtained gathering information from the 277 sheets of the Carta Geologica d'Italia, adopting a unique legend model to produce a homogeneous lithological map of the entire country.

However, specific applications in different geosciences fields require distinct criteria and methods to elaborate different lithological classifications. For example, starting from the geological maps produced by ISPRA at the 1:100,000 scale, a geo-lithological map of Italy was recently classified according to the expected seismic behaviour of the material (Forte et al. 2019), although the map is only represented as a figure along the paper, and not available for download or visualization.

Here, we describe a new lithological map of Italy (LMI), entirely available for download, aimed at differentiating lithotypes based on their expected geo-mechanical properties in relation to slope stability and with the specific purpose of being used in statistically based (Reichenbach et al., 2018; Schlogel et al., 2018; Alvioli et al., 2016; Rossi et al., 2016) and physically based (Alvioli et al., 2021, 2016; Mergili et al., 2014; Raia et al., 2013) slope stability models. Early versions of the map described in this work were used for geo-morphological analysis and terrain classification (Alvioli et al., 2020) and for rockfall susceptibility assessment (Alvioli et al., 2021). The map and the associated database were designed in a versatile way. They can be easily enhanced/reclassified using different or additional criteria, e.g., considering age, tectonic or geotechnical information, and thus can be relevant to a wide range of studies.

## 2 Data

LMI was prepared starting from the data of the 277 sheets of the geological map of Italy at 1:100,000 scale (Table 1, ID 6), provided by the Italian Institute for Environmental Protection and Research (ISPRA – Italian Geological Survey; *Servizio Geologico d'Italia*, 2004) available as a digital database through the ISPRA website. The website exhibits a representational state transfer (REST) service for the publication of spatial data (Table 1, ID 9), and distributes the geological map of Italy at a scale of 1:100,000, in vector format (Figure 1). The map contains 294,266 topologically correct polygons, and 5,477 unique descriptions of the geological formations. The scanned versions of the original geological sheets are also available for consultation (Table 1, ID 6).

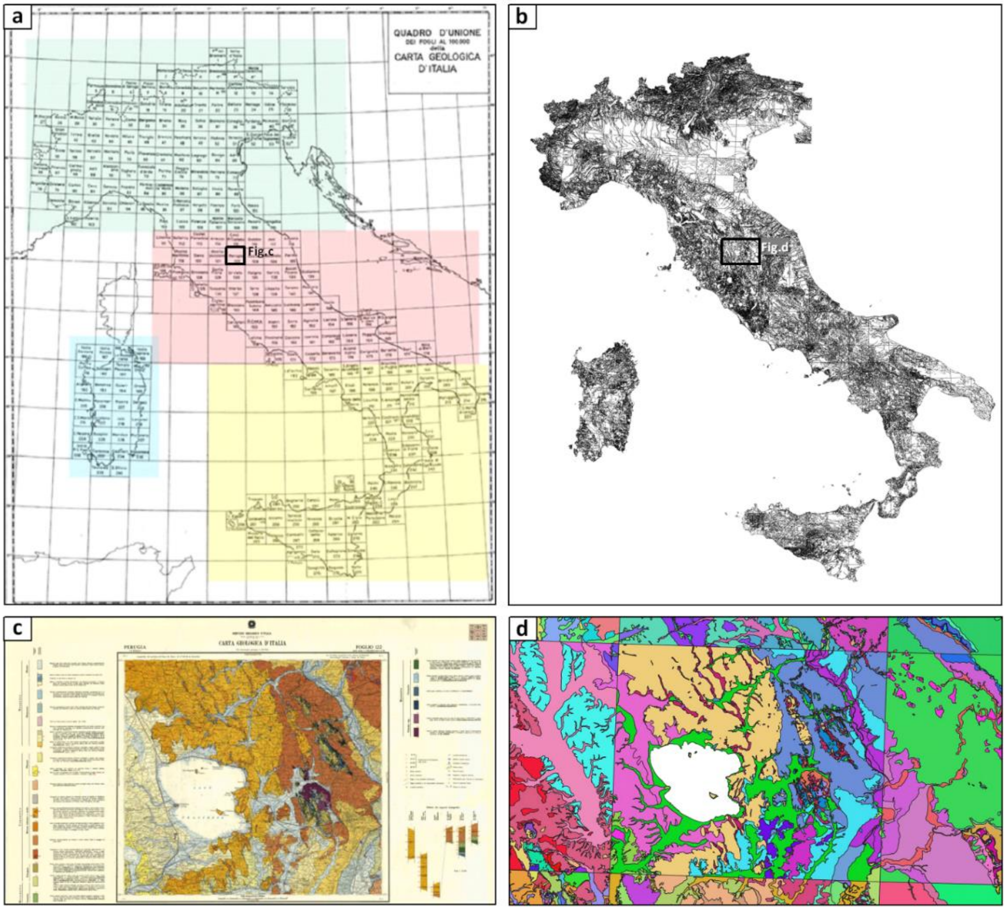


**Figure 1: (a)** The 277 sheets of the geological map of Italy at 1: 100,000 scale as visualized at the ISPRA website (Table 1, ID 6). The location of figure (c) is indicated; **(b)** All the unclassified 292,705 vector polygons available in the source dataset. The location of figure (d) is indicated; **(c)** Published version of the sheet n. 122 "Perugia" as visualized in raster form at the ISPRA website (Table 1, ID 6); **(d)** Randomly coloured polygons within the area encompassing the sheet n. 122. Polygons having the same geological description in the original attribute table (field: NAME) provided by ISPRA (Table 1, ID 9) assume the same colour. The area also encompasses the straight boundaries with its surrounding four geological sheets, clearly visible as sharp colour changes along NS and WE oriented straight lines.

The attribute table associated with the polygons originally contained a unique numeric identifier and the description of the geological unit as specified in the original geological maps (field: *NAME*). Comparison between the original legend descriptions and the text reported in the description field revealed that several simplifications were made. Such differences represented a major source of inhomogeneity within the database, which limited the efficacy of using automated database queries to apply the new lithological classification scheme. Table 2 reports examples of such simplifications of the original legend.

| **Simplifications and Problems in the Name_Ulf column** | **NAME Descriptions** | **Geological Sheet numbers** | **Approach to the issues** | **Original Descriptions** |
|---|---|---|---|---|
| *Lack of information concerning the name of the formation, the lithology and the internal architecture* | undifferentiated | 92-93 | SQ+ancillary | Sericitic, quartz-sericitic, chloritic schists, of Permian age, prevalent, not separable cartographically from schistose limestones because of the minute mixture determined tectonically |
| *Lack of information concerning the name of the formation and the lithology* | lenticular alternations | 130 | SQ+ancillary | Lenticular alternations, of variable extension and power, consisting of: clay and varicolored marl, calcarenite, calcareous breccia, sandstone, limestone and marly limestone. |
| *Lack of information concerning the lithology* | Corleto Perticara formation | 200 | SQ+ancillary | Violet, brown and yellowish clayeyes, gray and white clayey marls, subordinately red, calcareous marls and marly limestones of gray or greenish color, gray calcarenite or gray quartzarenites with siliceous cement. |
| *Only partial lithological information* | Corleto Perticara formation - marne | 199 | SQ+ancillary | Clayey marl gray and subordinately red; calcareous marl and marly limestone of gray or greenish color, calcarenite and sandstone. |
| *Identification of a rock unit with local/informal denomination* | “metallifero bergamasco”,<br><br>“biancone” | *7-18*<br><br>*35, 36, 49, 22,38* | SQ+ancillary | Well stratified black limestones, often with parallel lamination and pisolithic at the base; dolomite intercalations in the lower part.<br><br>White compact limestones; greyish or gray limestone; black marly, bituminous limestone; greenish marl; ceroid limestones with chert. |
| *Formations made up of several members* | sandstones, quartzites, phyllites, schistose sandstones, argilloscist | *226* | SQ+ancillary | Sandstones, quartzites, phyllites, schist sandstones, more or less philladic clayey, alternating, sometimes even minute. |
| *Typos* | “scisti di ?dolo” | 7-18 | Q | “Scisti di Edolo” |
| *Singular/plural* | moraine/moraines | 30, 31, 32, 17, 20, 12, 132, 140, 145, 151, 152, 160, 209, 210 /151 | Q | Moraine/Moraines |
| *Uppercase/lowercase* | Moraine/moraine | 62/25, 24, 22, 4[b], 22, 6, 8, 18, 19, 33, 34, 5, 15, 16, 27, 28, 29, 41, 55, 66 | Q | Moraine |

| | | | | |
|---|---|---|---|---|
| *Mangled names in some sheets* | "majolica" in place of "maiolica" | 139 | Q | "Majolica" |
| *Spelling errors* | "ammessi subvulcanici" | 11 | Q | "Ammassi subvulcanici" |
| *Use of accents* | "unità di sillano" | 108 | Q | "Unità di Sillano" |
| *Use of apostrophes* | "marne e calcari dell'antola" | 84, 85 | Q | "Marne e calcari dell'Antola" |
| *Use of percentage* | soils containing more than 10% of organic substances | 76 | Q | Soils containing more than 10% of organic substances |
| *Use of special character letters* | würmian moraines | 54, 42, 67, 4, 1-4ª, 14, 14ª, 91 | Q | Würmian Moraines |

**Table 2:** Examples of simplifications and problems related to the unique rocks descriptions contained in the source dataset, and comparison with the original description in the legend of the original geological sheets. Depending on their nature, issues were approached using database queries (Q), spatial queries (SQ), and ancillary material (regional/local geological maps and literatures).

In most cases, the text corresponds only to the first word or lemma of the original description. In the case of formations made up of several members, the *NAME* field contains a lemma indicating the main lithological members, but this approach is not consistent for all records. In some cases, the polygons correspond to empty records in the attribute table (most of them refer to lakes or inland waters); in others, the polygons are absent and were added in this work to fill in empty areas, according to the information checked in the original geological sheets. Overall, the analysis of the database revealed several types of errors affecting the source data set, which are summarized in Figure 2a. We refer to errors in the database as ***thematic errors***, since the attribute assigned to a polygon is incorrect or not corresponding to the ground truth (assumed here to be the original geological sheets). Thematic errors in the database can be grouped according to two main categories: *inconsistency between surveyors*, and *errors of the operators* who compiled the database. We refer to the first as to "*Data acquisition errors*" and to the second as to "*Database compilation errors*".

*Data acquisition errors* are related to individual mapping errors (*Reconnaissance errors*, in Figure 2a) or to disused, or dialectal/jargon geological descriptions (*Semantic errors*, in Figure 2a). Figures 3a and 3c show typical errors related to subjectivity issues visible at the boundary between geological sheets drafted by different working groups and published many years apart from each other (Console et al. 2017). Figure 3c also contains references to local or dialectal terms that may escape general lithological classification criteria. Subjectivity errors related to disused, inadequate or dialectal geological description and terms were systematically resolved (Figure 3d) by using database queries. Despite our effort, little or nothing could be done for most of the errors due to contrasting classification of rock assemblages by individual geologists or the working groups who compiled the original geological sheets. Such problems still remain in our lithological map (Figures 3b,d). A new national geological survey currently in progress (Carg project, Table 1, ID 7, 8) will likely resolve critical information of geological interpretation, which is beyond the scope of this work.

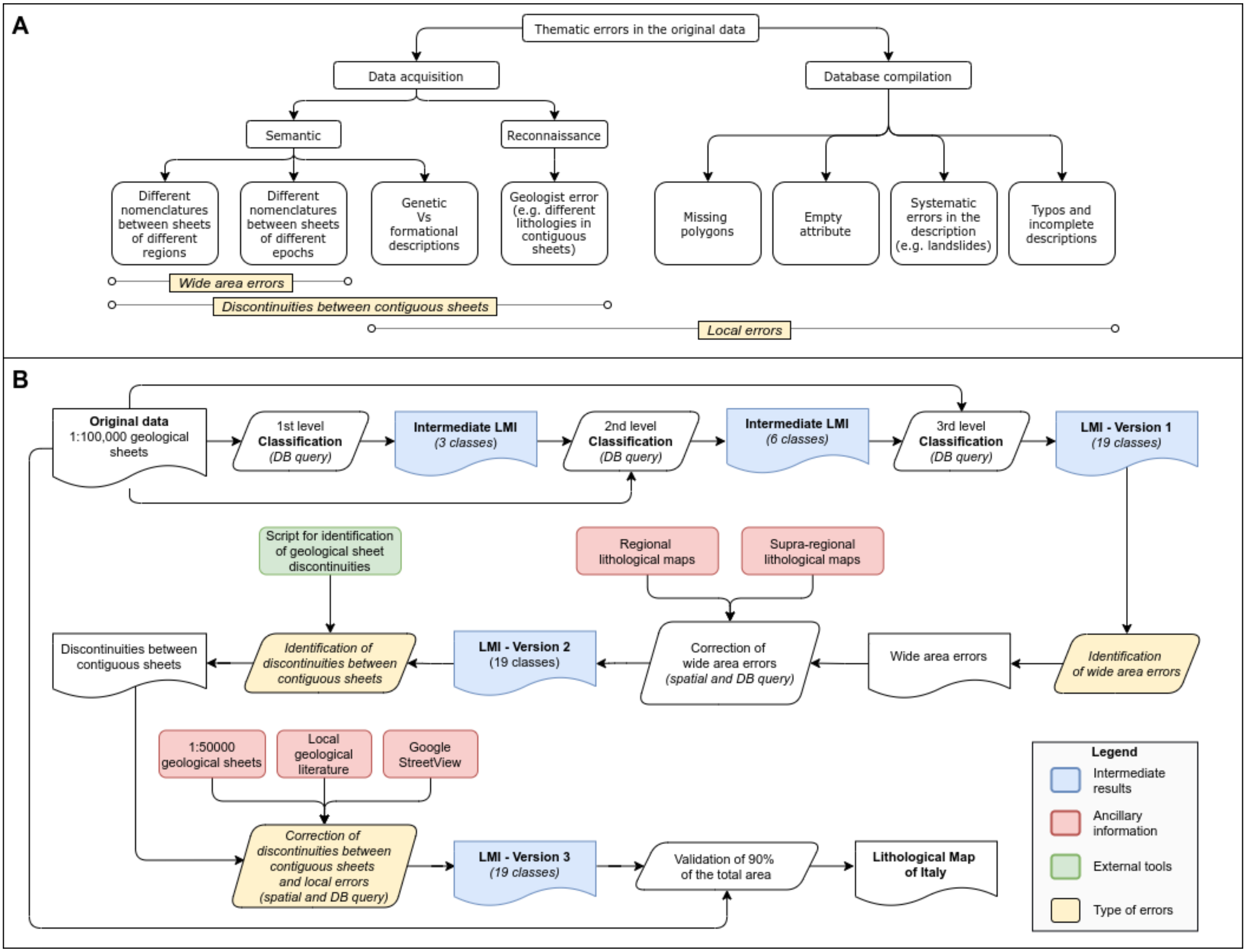


**Figure 2: (a)** Scheme of the main thematic errors identified in the source dataset. Errors can be related to (i) uncorrected or incomplete database compilation or (ii) to data acquisition as a consequence of individual errors or inhomogeneity in the use of geological nomenclature, description and interpretation; **(b)** Flowchart of the classification process of the Lithological Map of Italy

*Database compilation errors* can be systematic (Figure 3f) and occasional. Figure 3f refers to a systematic thematic error dealing with the compilation of the *NAME* column of some landslide polygons with the description of a lithostratigraphic unit clearly unrelated to landslides. As exemplified in Figure 3f, the compilation errors were identified and corrected during the reclassification of the source dataset.

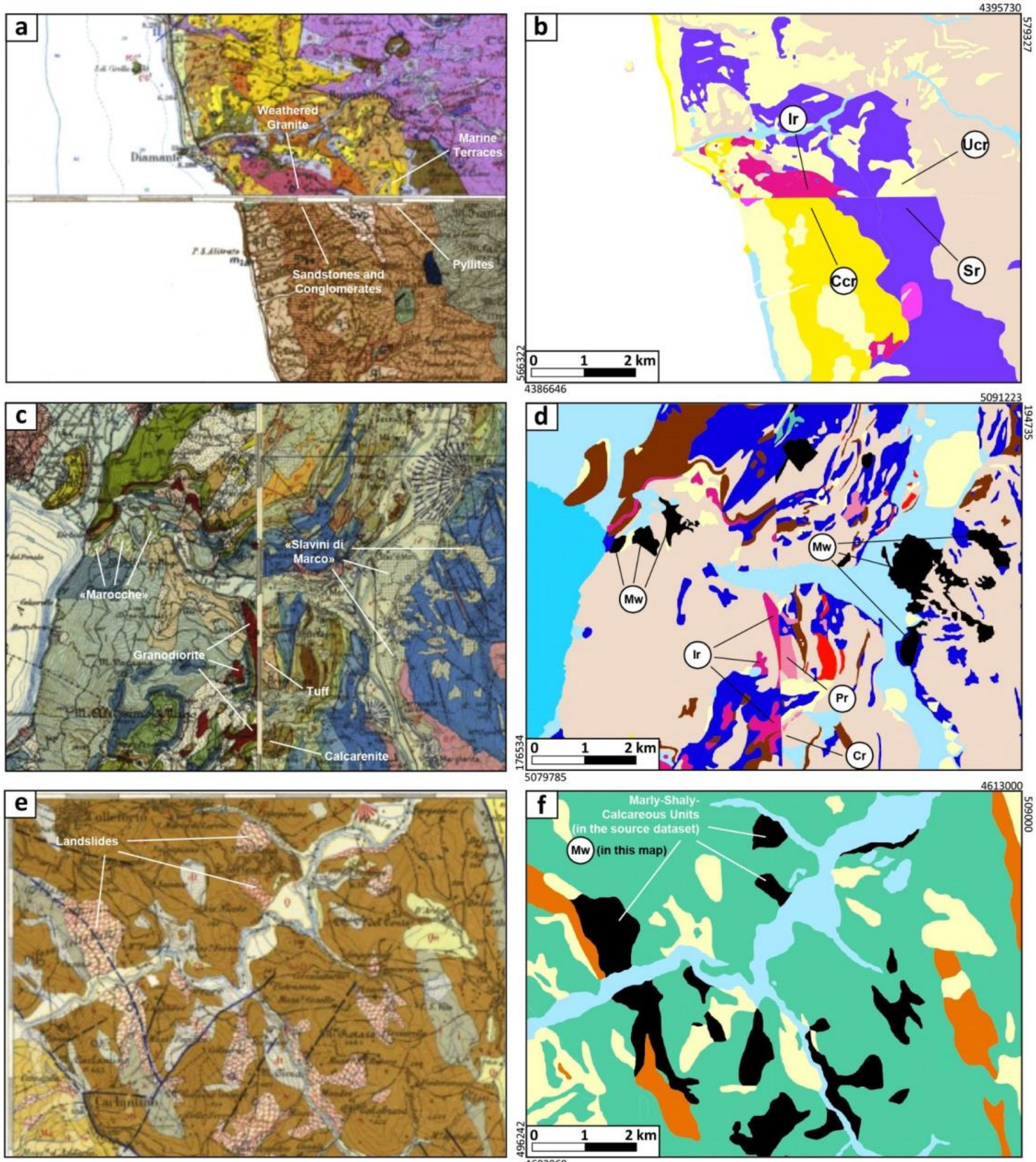


**Figure 3:** Main problems of the source dataset highlighted through the comparison of representative areas, as appear respectively in the published raster version of the geological sheets **(a, c, e)** and in the our reclassified vector map (LMI) **(b, d, f)** - Vector Map Legend - Ir (Intrusive rocks), Ucr (Unconsolidated clastic rocks), Ccr (Consolidated clastic rocks), Sr (Schistose rocks), Pr (Pyroclastic rocks), Cr (Carbonatic rocks), Mw (Mass wasting); Example of errors related to locally wrong rocks classification and inhomogeneity problems at the boundary between geological sheets of different years are shown in (a) (year 1969 - N sheet n. 220 vs year 1890 - S sheet n. 228) and in (c) (year 1948 - W sheet n. 35 vs year 1966 - E sheet n. 36); Examples of local/dialectal terms in the geological description are shown in (c) (“Marocche” and “Slavini di Marco” for Mass wasting); Examples of errors related to incorrect database compilation are shown comparing (e) and (f). Figures **a, c, e,** include sheets number **220, 228, 35, 36, 163** as visualized in raster form at the ISPRA website (Table 1, ID 6).

## 3 Methods

The procedure used to compile out the new Lithological map of Italy (LMI) is described in Figure 2b. Starting from the original data (top left in Figure 2b) we derived the LMI (bottom right in Figure 2b) through the following steps: (a) definition of a procedure including alphanumeric queries, geospatial analysis and expert judgements; (b) preparation of at least two intermediate products and three versions of the LMI.

The "*Intermediate LIM - 3 classes"* product (Figure 2b) follows a genetic criterion and describes (i) magmatic, (ii) metamorphic and (iii) sedimentary rocks.

The "*Intermediate LIM - 6 classes"* product (Figure 2b), distinguishes (i) older (typically Pre-Neogene in age) and structured substratum-derived sedimentary rocks and (ii) magmatic intrusion, from (iii) younger (Neogene and Quaternary in age) less-to-not deformed sedimentary and magmatic cover rocks. Sedimentary cover was further separated in (iv) undifferentiated and (v) alluvial/marine rocks, while the (vi) metamorphic rocks class remains unchanged.

"*LMI - Version 1*" (Figure 2b) is based on a predominantly lithological criterion, and contains the 19 classes defined in our legend.

To translate different rock type information into lithological classes, the dominant rock types were emphasized assuming that rocks mentioned foremost are more abundant than those mentioned later in the descriptions. This classification strategy is consistent with many mapping guidelines (UNESCO-IUGS, 2016; Hartmann et al., 2012; Asch, 2005), and is based on the classification system by Dürr at al. (2005), with modifications. Determining the dominant rock types within a unit was not always straightforward, though. Cases of uncertainty about the dominant rock type were found and were resolved by considering specific lithological classes defined by the combination of the most representative rock types. For example, the rock unit named "Clays and Limestones", composed in equal parts of both lithotypes, was assigned to the class "mixed sedimentary rocks", which also contains other sediments where carbonates are mentioned but not dominant.

Each classification step ("1st, 2nd, 3rd level" in Figure 2b) used the result of the former step (where applicable) and the original data to build complex alphanumeric database queries. No spatial queries were involved. Furthermore, the first two (coarser) levels of classification (intermediate products) helped underlining systematic semantic and compilation errors throughout the database. For example, rock units containing the word "schist" were consistently classified as "metamorphic rocks" in the first level classification, which led to classifying sedimentary rocks with a strong pelitic component as metamorphic rocks. This happened since such sedimentary rocks were commonly improperly indicated as "schists" in geological descriptions dating over 50 years. Similarly, the words "clays" and "claystones", or "sands" and "sandstones", were sometimes used as synonyms in the original geological legend, with consequent uncertainty between the sedimentary cover or the sedimentary substratum.

Inconsistencies of the source data set mainly derive from the large variability of the level of detail of the original geologic descriptions between different geological sheets. Compilation of the 277 geological sheets of the entire National territory required 92 years, from 1884 to 1976 (Figure 4a), which inevitably led to differences in the geological descriptions (and interpretation) between old and recent sheets.

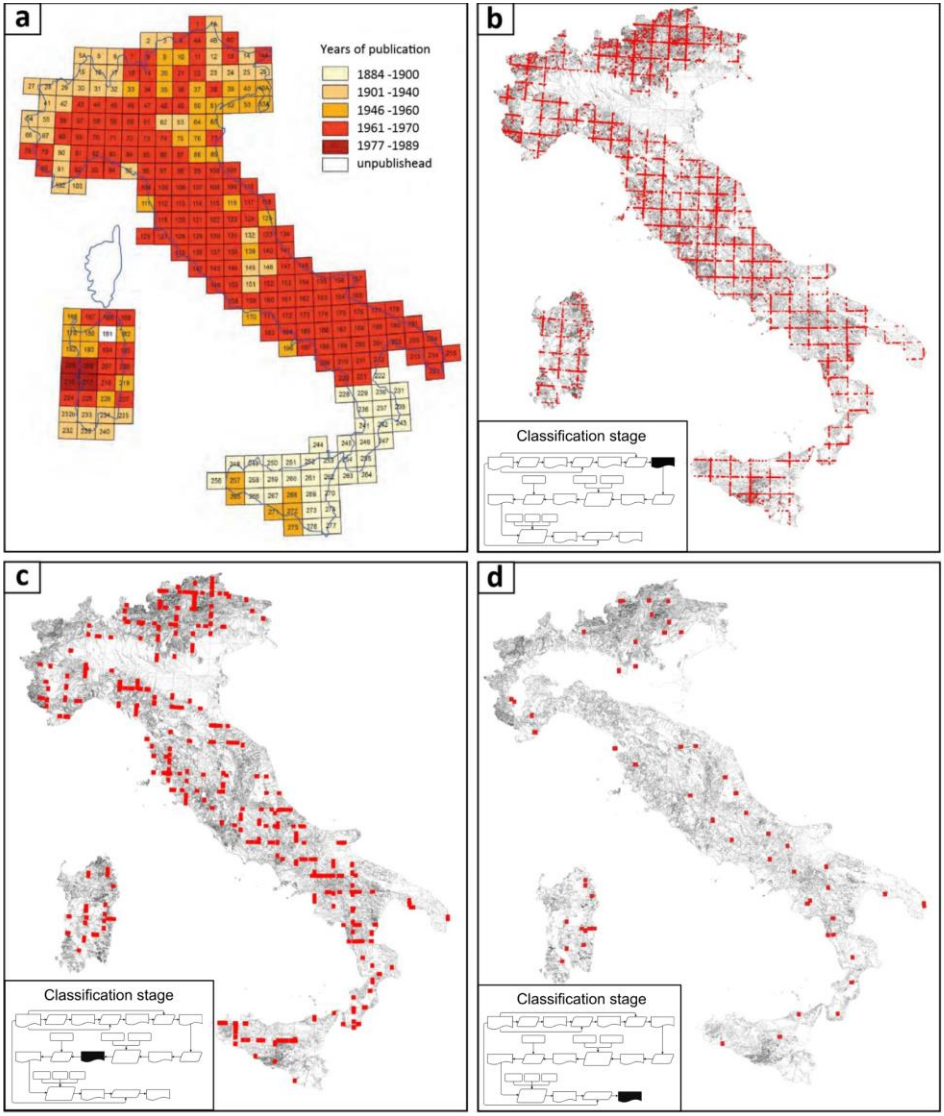


**Figure 4:** (a) The 277 sheets of the geological map of Italy at 1: 100,000 scale classified according to the years of publication, as visualized in Console et al., 2017, Figure 3; (b) The 12711, NS-EW oriented segments (red lines) having different lithotypes in the two sides and sinuosity equal to 1. (c) The 405 Red lines longer than 1000 m left after semi-automatic classification. The unclassified 294,266 vector polygons of the source dataset are shown as background in (b) and (c); (d) the 58 Red lines longer than 1000 m left after the expert analysis of the semi-automatic output. The unclassified 100,705 vector polygons derived from the dissolve GIS operation performed after the classification phase are shown as background. Insets in (a), (b), and (c) indicate the classification stage to which each map refers, according to the scheme in figure 2b.

A similar issue was introduced between sheets or regions mapped by different authors and working groups (Figures 3a,c). As a consequence, problems of inhomogeneity were found in the descriptions of litho-stratigraphic units, which in turn generated problems of harmonization at the boundary between different geological sheets. To mitigate inhomogeneity problems, we decided to adopt broad categories in the classification of the third level as a function of similar lithology, genetic processes and expected geotechnical behaviour. With this aim, rock descriptions were generalized into 19 lithological classes. However, harmonizing the original 5,477 univocal descriptions of the geological units in 19 simplified lithological classes was often tricky and required expert judgement supported by the consultation of regional and supra-regional geo-lithological maps (Conti et al., 2020; Piana et al., 2017; Lentini & Carbone, 2014; Carmignani et al., 2013; Vezzani et al., 2010; Celico et al., 2005; Carmignani, 2001; Consiglio Nazionale delle Ricerche, 1990; Amodio Morelli et al., 1976). We used a very long and complex set of database queries to classify and harmonize the data. For example, to correctly classify glacial drift avoiding possible overlapping with alluvial deposits, we requested the NAME field to either contain strings with the words "wurm", "würm", "glacial", "moraine", and at the same time without any of the words "alluvial", “fluvial” and “terrace”. Due to their specificity, queries were generally longer and more complex when used to classify widespread lithological classes containing a large number of unique descriptions. The *LMI - Version 2* is the product of this harmonization phase where “wide area errors” were corrected (Figure 2b), resulting in a lower number of discontinuities at the boundaries of regions or individual geological sheets, compared to these contained in the *LMI _Version 1* (Figure 4 b,c).

To identify discontinuities between contiguous geological sheets (Figure 2b) we developed an automatic procedure based on the analysis of the lithological classes located to the right and left of each lithological boundary. We selected all EW and NS oriented straight boundaries longer than 1 km and resolved classification inconsistencies across such boundaries by expert advice. Discontinuities between contiguous geological sheets are due to inconsistencies between surveyors. Since we assumed that the ground truth is the original geological sheets, our approach consisted in assuming only one of the two contiguous polygons was to be corrected. If available ancillary data allowed to confirm one of the two bounding polygons attribute, classification of the second polygon was amended accordingly. Otherwise the discontinuity was solved by assigning the class that minimised discontinuities and inconsistencies.

To reduce the number of discontinuities between contiguous sheets, we consulted geologic maps available at the 1:100,000 scale (Servizio Geologico d’Italia, 1970a,b,c,d,e, 1969, 1968a,b, 1965, 1964, 1955; Ministero dei Lavori Pubblici, Ufficio Idrografico, Sezione Geologica, 1948; R. Ufficio Geologico, 1884a,b,c,d,e, 1900) and at the 1:50,000 scale (Servizio Geologico d’Italia, 2016, 2015a,b,c, 2014, 2012a,b,c, 2011a,b,c,d, 2010a,b,c, 2009a,b, 2008, 2006, 2005a,b,c,d, 2002, 1973, 1972), where available. Where information on rock types was unavailable from the national maps, we obtained the descriptions of the named stratigraphic units from regional and local geological maps and from the scientific literature (Novellino et al., 2021; Bucci et al., 2020, 2016, 2014, 2012; Vignaroli et al., 2019; Mirabella et al., 2018; Ronchi et al., 2011; D’Ambrogi et al., 2010; Brozzetti, 2007; Chiarini et al., 2008; Giannandrea et al., 2006; Schiattarella et al., 2005; De Rita et al., 2004; Girotti

& Mancini, 2003; Catanzariti et al., 2002; Bortolotti et al., 2001; Prosser, 2000; Giardino & Fioraso 1998; Tavarnelli, 1997; Campobasso et al., 1994; Centamore et al., 1991; Patacca et al., 1991; Calamita et al., 2009; Centamore et al., 2009; Gueguen et al., 2010; Tavarnelli et al., 2003a, b). The quality of the literature was variable, and may have introduced some uncertainty. In some rare locations, the rock type information of digital geological map vector datasets was derived from paper maps, which were georeferenced and visually assigned to the units of the digital maps. In specific and rare cases, it was necessary to use geographic visualization software, such as Google Earth and Google Street View, to study and display images of outcrops for a local visual analysis. After this finer phase of correction, a total of 58 segments longer than 1000 m remained unsolved since they would require the geometry of the original polygons to be modified (Figure 4d). The problem greatly increases for the classification inconsistencies along segments shorter than 1,000 meters, for which a systematic correction was out of the scope of this work.

After the classification phase, boundaries were dissolved to merge adjacent polygons sharing the same lithology. With this streamlining operation, the number of polygons has dropped from 294,266 to 180,503. The result of the correction of discontinuities between contiguous sheets is the *LMI - Version 3* (Figure 2b).

Eventually, we performed a validation of the map *LMI – Version 3* (Figure 2b). First, the area percentages of all the unique descriptions within each class were computed and sorted in descending order. Then, within each lithological class, all the unique descriptions summing to a total area of 90% of that class were inspected for possible inconsistencies, by comparing and verifying the assigned lithology with the original description in the field NAME. The total area validated corresponds to 271,651.56 km$^2$, which represents ~90% of the Italian territory and includes 1,702 different geological descriptions. For each lithological class, polygons of a very small size, between 0.05% and 0.8% of the area of the lithological class itself, were validated (Table 3). The remaining 10% of the total area of each lithological class, which consists of 4,632 records associated with negligible percentage values of the area (on average 0,06% of the total area of each class), was not checked. It is worth noting (Table 3) that the Carbonate rocks class (Cr) accounts for most of the descriptions (1,155), followed by Unconsolidated clastic rocks (Ucr), Alluvial and marine deposits (Al) and Siliciclastic sedimentary rocks (Ssr) which include 856, 583 and 560 descriptions respectively. However, the areal extent of these four classes (the most represented on the territory) does not reflect the number of descriptions, as the most extensive class is Al (75,424.36 km$^2$), followed by Ucr (45,764.12 km$^2$) and then Cr and Ssr (45,329.81 km$^2$ and 34,099.68 km$^2$, respectively).

We checked all of the records classified as anthropogenic deposits (12 records), landslides (26 records), lakes and glaciers (10 records) (Table 3). Some errors inherited from compilation errors of the source dataset, also emerge from the validation as classification inconsistencies. To give an example of this kind of errors we report a case from the landslide class, in which the most representative (21% of the area, with respect to the total landslide class) unique descriptions are defined as “clayey and calcareous turbidites of Paleogene age”. These same polygons were, instead, correctly represented as landslides in the original geological sheet in raster format (Figure 3e). Wherever possible, polygons classified as landslides were manually corrected by looking at the original raster map. Similar errors concerning other geological descriptions were treated using the same approach. After validation, the final *Lithological Map of Italy* (LMI) was produced (Figure 2b).

| **Lithologic class** | **N. object (#)** | **A. min ($m^2$)** | **A. max ($km^2$)** | **A. med ($km^2$)** | **A. tot ($km^2$)** | **N. description (#)** | **N. description checked (#)** | **A. description checked (%)** | **A. min checked (%)** |
|---|---|---|---|---|---|---|---|---|---|
| *Sr* | 13,040 | 50 | 1909.83 | 1.32 | 17,296.50 | 436 | 93 | 90 | 0.18 |
| *Nsr* | 14,595 | 263 | 994.09 | 0.64 | 9351.25 | 382 | 100 | 90 | 0.17 |
| *Ir* | 11074 | 56 | 4238.05 | 0.97 | 10,778.27 | 363 | 55 | 90 | 0.22 |
| *Pr* | 5508 | 239 | 2447.07 | 1.66 | 9121.65 | 360 | 112 | 90 | 0.18 |
| *Lb* | 7735 | 259 | 1227.15 | 0.81 | 6256.87 | 336 | 85 | 90 | 0.21 |
| *Cr* | 21,070 | 16 | 4836.92 | 2.15 | 45,329.81 | 1155 | 304 | 90 | 0.05 |
| *M* | 8541 | 23 | 243.65 | 0.70 | 5964.80 | 235 | 78 | 90 | 0.21 |
| *SM* | 5382 | 216 | 921.16 | 1.57 | 8455.40 | 181 | 66 | 90 | 0.35 |
| *Cm* | 4167 | 58 | 911.52 | 1.62 | 6752.96 | 114 | 25 | 90 | 0.67 |
| *Ssr* | 11,930 | 24 | 3924.31 | 2.86 | 34,099.68 | 560 | 145 | 90 | 0.12 |
| *E* | 2634 | 989 | 238.72 | 0.70 | 1839.48 | 87 | 22 | 90 | 0.72 |
| *Ucr* | 37,,641 | 32 | 1260.33 | 1.22 | 45,764.12 | 856 | 229 | 90 | 0.08 |
| *Ccr* | 8391 | 39 | 1392.17 | 1.66 | 13,915.05 | 397 | 112 | 90 | 0.16 |
| *Gd* | 11337 | 2145 | 318.28 | 0.74 | 8406.20 | 107 | 16 | 90 | 0.63 |
| *Mw* | 1231 | 33 | 9.18 | 0.26 | 315.72 | 26 | 26 | 100 | 0.02 |
| *Ad* | 125 | 1573 | 25.31 | 0.71 | 88.72 | 12 | 12 | 100 | 0.03 |
| *Li* | 329 | 1252 | 367.79 | 4.52 | 1485.44 | 10 | 10 | 100 | 0.01 |
| *B* | 968 | 136 | 105.96 | 1.01 | 978.80 | 79 | 35 | 90 | 0.60 |
| *Al* | 14,804 | 66 | 46,634.58 | 5.09 | 75,424.36 | 583 | 177 | 90 | 0.10 |

**Table 3:** Descriptive statistics of the 19 lithological classes. In the left half of the table, the number of polygons, and their minimum, maximum, average and total area for each lithological class are shown. The right half of the table shows the number of total unique descriptions and those checked during the technical validation in relation to the percentage of the area covered by the validation (% of the total area) and the detail of the validation (minimum area checked)

## 4 Results

The main results of this work are: (i) the translation of the rock type information extracted from the stratigraphic units of the geological maps of Italy at the 1:100,000 scale into lithological classes and (ii) the development of a data architecture open to further improvement, aimed in particular at linking the lithological classes to their expected geotechnical behaviour.

The new *Lithological map of Italy* (LMI, this work) represents the first freely downloadable national distribution of the different lithological classes at a high resolution. The dataset is publicly available at https://doi.org/10.1594/PANGAEA.935673 (Bucci et al. 2022). The map scale is 1:100,000. The assembled map consists of a total of 180,503 polygons distributed in 19 lithological classes (Figure 5).

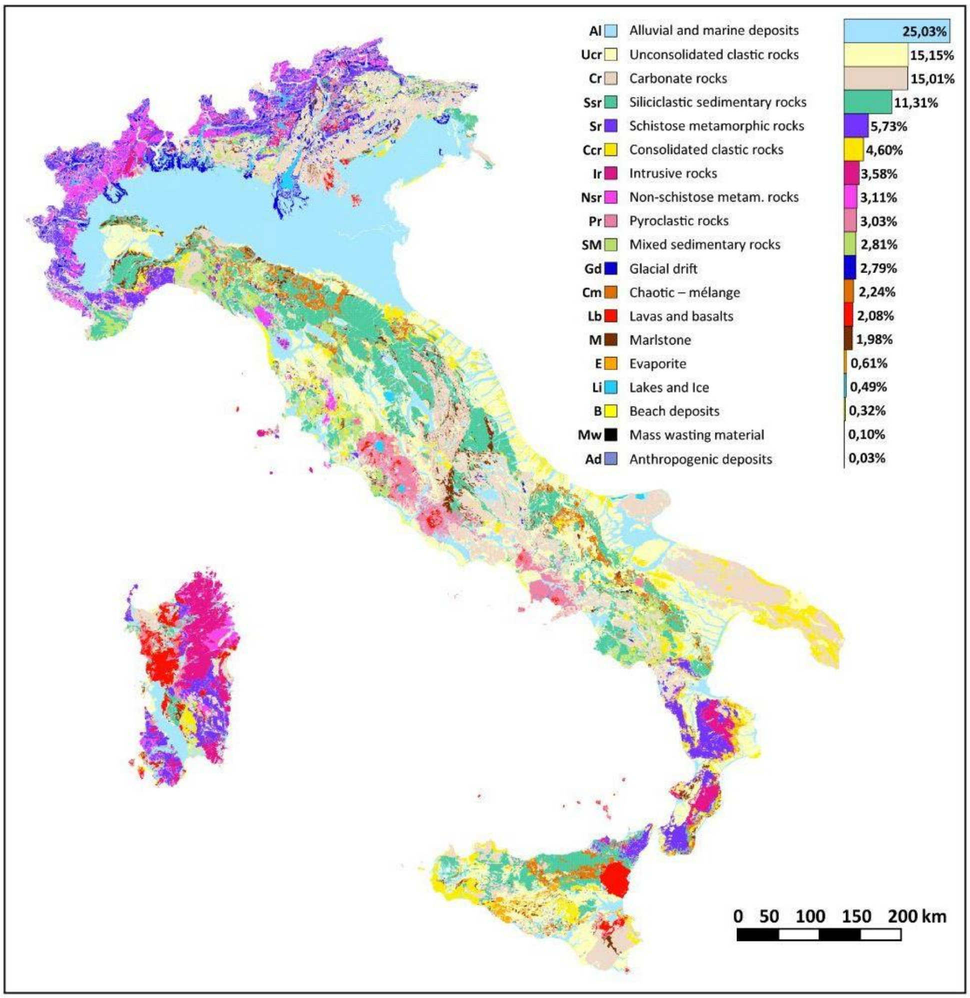


**Figure 5:** Map of Italy showing the 19 lithological classes identified both with the short ID and the extended name. Percentage distribution of each lithological class over the Italian territory is indicated and visualized in a bar chart.

The Italian surface is covered by 82,47% sediments (a third of which are alluvial deposits), 8,84% metamorphics, 3,58% plutonics, and 5,11% volcanics (Table 4). A specific class was assigned to areas of ice and inland water bodies, which cover 0,49% of the map area.

| Physiographic regions of Italy | | Metamorphic | | Magmatic | | | Sedimentary | | | | | | | | | | | | | | ← I level |
|---|---|---|---|---|---|---|---|---|---|---|---|---|---|---|---|---|---|---|---|---|---|
| Acronym | Name | Substratum | | Intrusion | Cover | | Substratum | | | | | Undifferentiated Cover | | | | | | Alluvial/ Marine | | | ← II level |
| | | Sr | Nsr | Ir | Pr | Lb | Cr | M | SM | Cm | Ssr | E | Ucr | Ccr | Gd | Mw | Ad | Li | B | Al | ← III level |
| EAL | *Eastern Alps* | 1.7 | 0.2 | 0.9 | 4.0 | 2.7 | 46.5 | 2.2 | 5.7 | - | 4.5 | 0.1 | 10.3 | 1.4 | 9.7 | 0.3 | - | - | 0.7 | 9.3 | 100 |
| CAL | *Central Alps* | 15.8 | 13.8 | 4.5 | 1.7 | 0.6 | 21.1 | 1.0 | 3.2 | - | 2.4 | 0.0 | 10.3 | 0.5 | 15.8 | 0.3 | - | - | 2.7 | 6.2 | 100 |
| WAL | *Western Alps* | 26.7 | 25.2 | 4.9 | 0.1 | 0.1 | 6.4 | 0.5 | 3.1 | 0.0 | 4.8 | 0.0 | 8.3 | 2.1 | 11.0 | 0.0 | 0.0 | - | 0.7 | 6.0 | 100 |
| PP | *Po Plain* | 0.0 | 0.1 | 0.1 | 0.2 | 0.1 | 0.2 | 0.1 | - | 0.0 | 0.4 | 0.0 | 1.7 | 0.4 | 3.6 | - | 0.2 | 0.0 | 0.5 | 92.5 | 100 |
| NAP | *Northern Apennine* | 1.0 | 1.5 | 0.2 | - | 0.0 | 6.7 | 5.6 | 9.6 | 10.2 | 39.0 | 0.7 | 11.3 | 3.3 | 0.3 | 0.2 | 0.0 | - | - | 10.3 | 100 |
| NIAP | *North-Internal Apennine* | 0.7 | 1.3 | 0.6 | 1.7 | 0.3 | 6.1 | 1.3 | 8.9 | 1.1 | 18.6 | 0.4 | 28.2 | 4.8 | - | 0.1 | 1.5 | 0.1 | 0.6 | 23.7 | 100 |
| CEAP | *Centre-Eastern Apennine* | - | - | - | - | - | 1.0 | 0.6 | - | 0.1 | 12.0 | 0.3 | 51.1 | 11.2 | - | 0.0 | 0.5 | - | - | 23.2 | 100 |
| CAP | *Central Apennine* | - | - | - | 3.1 | 0.1 | 47.6 | 9.4 | 0.0 | 0.0 | 14.7 | 0.0 | 11.4 | 2.2 | 0.4 | 0.0 | 0.0 | 0.0 | 0.1 | 10.9 | 100 |
| CMP | *Central Magmatic Province* | 0.0 | - | - | 58.4 | 9.3 | 3.4 | 0.1 | 0.4 | - | 0.2 | 0.0 | 13.0 | 0.8 | - | 0.0 | 0.0 | 0.0 | 3.0 | 11.3 | 100 |
| SMP | *Southern Magmatic Province* | - | - | - | 50.1 | 3.8 | 10.3 | 0.0 | - | 0.1 | 3.9 | - | 21.9 | 0.0 | - | - | 1.5 | 1.6 | 0.1 | 6.6 | 100 |
| SAP | *Southern Apennine* | 1.8 | 0.1 | 0.0 | 1.9 | 0.1 | 20.0 | 1.5 | 5.8 | 7.4 | 24.8 | 0.1 | 21.9 | 5.9 | 0.0 | 0.6 | 0.1 | - | 0.0 | 8.0 | 100 |
| SEAP | *South-Eastern Apennine* | - | - | - | - | - | 1.3 | 0.0 | 0.0 | 0.3 | 0.3 | 0.0 | 51.6 | 7.8 | - | 0.0 | 1.1 | - | 0.6 | 36.9 | 100 |
| GF | *Gargano Foreland* | - | - | - | - | - | 79.3 | - | - | - | - | - | 4.8 | 0.3 | - | - | 0.4 | - | 3.8 | 11.4 | 100 |
| MF | *Murge Foreland* | - | - | - | - | - | 59.7 | - | - | - | - | - | 12.1 | 24.4 | - | - | 0.2 | - | - | 3.6 | 100 |
| WS | *Western Sicily* | 0.1 | - | - | 0.0 | 0.0 | 10.0 | 2.5 | 0.4 | 7.0 | 26.6 | 6.5 | 24.1 | 13.6 | - | 0.0 | 0.1 | - | 0.0 | 9.0 | 100 |
| ES | *Eastern Sicily* | - | - | - | 2.8 | 21.8 | 27.1 | 2.4 | - | 0.5 | 1.7 | 0.9 | 25.0 | 3.5 | - | - | 0.3 | - | - | 14.1 | 100 |
| CPA | *Calabro-Peloritano Arc* | 29.0 | 0.2 | 14.4 | 0.3 | 0.3 | 2.4 | 2.7 | 0.0 | 2.3 | 4.8 | 2.2 | 22.2 | 9.0 | - | 0.0 | - | - | - | 10.3 | 100 |
| SB | *Sardinian Block* | 15.7 | 5.6 | 26.6 | 4.3 | 13.5 | 7.0 | 0.9 | - | 0.0 | 3.2 | - | 3.2 | 2.8 | - | - | 0.6 | 0.0 | 0.1 | 16.5 | 100 |
| Total Italian territory **III level** → | | **5,73** | **3,11** | **3,58** | **3,03** | **2,08** | **15,01** | **1,98** | **2,81** | **2,24** | **11,31** | **0,61** | **15,15** | **4,60** | **2,79** | **0,10** | **0,03** | **0,49** | **0,32** | **25,03** | 100 |
| Total Italian territory **II level** → | | **8,84** | | **3,58** | **5,11** | | **33,35** | | | | | **23,28** | | | | | | **25,84** | | | 100 |
| Total Italian territory **I level** → | | **8,84** | | **8,69** | | | **82,47** | | | | | | | | | | | | | | 100 |

**Table 4:** Percentage distribution of the lithological classes (columns), organized in three hierarchically different levels of classifications, within the 18 physiographic regions of Italy (rows).

Below, the lithological classification describes the general rock types in each unit, in alphabetic order.

- **Alluvial deposits (Al)**: alluvial, lacustrine, swamp and marine deposits. Eluvial and colluvial deposits.
- **Anthropogenic deposits (Ad)**: include Roman and modern landfills, drainage channel excavations and archaeological remains.
- **Beaches and coastal deposits (B)**: include beaches and coastal deposits.
- **Carbonate rocks (Cr)**: carbonate-dominant sedimentary rocks. Examples of Cr units are limestone, dolomite and marl (but only where associated and in a clear minority with respect to limestone, otherwise they are included in class M). As usually the rock descriptions of the mapped units do not give relative abundances of the rock types which they encompass, units were classed as Cr if the first named rock type was a carbonate rock, if the majority of rock types were carbonates or if the named order otherwise led to the impression of a domination by carbonates.

- **Chaotic – mélange (Cm)**: include chaotic terrains with a predominantly clay matrix and olistostromes composed by mixed sedimentary rocks (SM class). Fragments of ophiolite structures were locally included in the Cm class.
- **Consolidated clastic rocks (Ccr)**: clay, sand, debris, conglomerates with a varied origin, usually of Neogene and Quaternary age, which have undergone consolidation or secondary cementation phenomena.
- **Evaporite (E)**: contains substantial amounts of evaporitic rocks. The typically and most frequently encountered evaporite rock is gypsum, but also anhydrite and halite are present. If a map unit was interpreted as dominated by evaporites, it was classified as E, regardless of other mentioned rocks. This implies that E class may additionally contain, e.g., carbonates.
- **Glacial drift (Gd)**: include moraines and other related deposits.
- **Intrusive rocks (Ir)**: acid (granites, quartz-diorites, quartz-monzonites), intermediate (diorite, monzonite, syenite), and basic (gabbros and peridotites) plutonics. Ophiolite structures are included into basic plutonic except for basalt (Lb class) and serpentinite (Sr class).
- **Lakes and Ice (Li)**: lakes, rivers, ice and glaciers on some Alpine mountains. However, the coverage is not representative for a lake or ice extent, as the priority of this map is on lithology.
- **Lavas and basalts (Lb)**: volcanic rocks including acid (rhyolites, trachytes or dacites), intermediate (andesites) and basic (basalt-type rocks, tephrites, tholeites and lamprophyres) volcanics.
- **Marlstone (M)**: includes mostly marly rocks with a composition ranging from calcareous marls to clayey limestones. Typically, it contains marly sediments of cartographic importance associated with Carbonatic rocks (Cr) or Siliciclastic sedimentary rocks (Ssr).
- **Mass wasting material (Mw)**: include landslides.
- **Mixed sedimentary rocks (SM)**: sediments where carbonate is mentioned but not dominant. The class encompasses mixed sedimentary rocks that are usually a combination of different rock types (e.g., interlayered sandstone and limestone, or shaley marl with interlayered subordinated calcilutite beds or radiolarite). Mixed pelagic sediments as well as calcareous turbidites are included in the SM class.
- **Non-schistose metamorphic rocks (Nsr)**: metamorphics where schistose fabric can be present but not dominant. It contains gneiss, amphibolite, quartzite, meta-conglomerate, and marble.
- **Pyroclastic rocks (Pr)**: sediments of volcanic origin. Typical pyroclastics are tuff, volcanic breccias, ash, slag, pozzolane, pumice.
- **Schistose metamorphic rocks (Sr)**: 'broad' lithological class that encompasses a wide variety of rocks from phyllite to schist, including association of schist and paragneiss. Ophiolite derived rocks that show a certain degree of metamorphism and schistosity (e.g. Serpentinite) are included in this class
- **Siliciclastic sedimentary rocks (Ssr)**: sandstone, mudstone and greywacke. Where carbonate was named in the rock description of the mapped unit, the lithological classes Cr or SM was used, so siliciclastic sedimentary rocks are without

mapped carbonate influence. Note that in some cases the carbonate presence (e.g., as matrix) may not be named in the rock description, and siliciclastic sediments may still contain carbonate in nature.

- **Unconsolidated clastic rock (Ucr)**: young, not yet consolidated and/or weathered sediments, usually of Neogene and Quaternary age. It comprises all grain sizes with a heterogeneous origin loosely arranged and not cemented together. Examples of unconsolidated sediments are clay soil, sand, not cemented breccia, loose debris and conglomerate.

Significant regional differences in the distribution of lithologies exist (Figure 6a,b,c, Table 4).

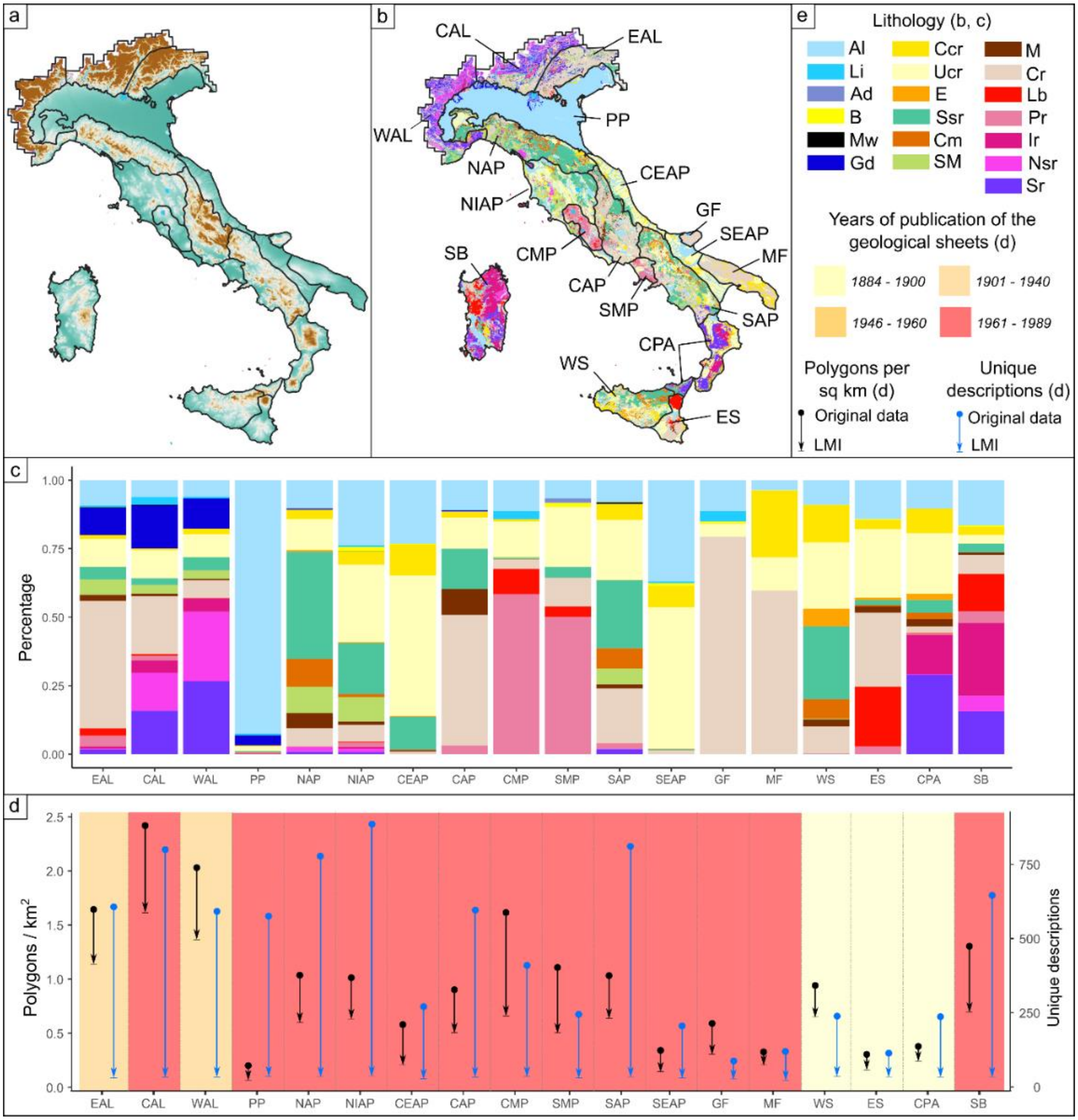


**Figure 6: (a)** Physical map of Italy subdivided into 18 physiographic regions; **(b)** Geographical distribution of the identified 19 lithological classes in the 18 physiographic regions of Italy (see Table 4 for spelling out the acronyms); **(c)** Percentage distribution of the 19 lithological classes in each physiographic region; **(d)** Polygons density (black symbols) and number of unique description (blue symbols) in each

physiographic region considering the original data (points) and the LMI (arrow tips), and taking into account the years of publication of the geological sheets; **(e)** Legend. See Figure 5 for the extended lithological legend.

With the exception of flat and low-lying areas of Italy, where alluvial deposits and loose clastic deposits dominate (e.g. Po Plain, PP), the map shows a high regional lithological variability. In the Western Alps (WAL) metamorphic rocks dominate while in the Eastern Alps (EAL) carbonate rocks prevail. Intermediate percentages are recorded in the Central Alps (CAL), where the metamorphic rocks to the N-NW and the sedimentary rocks to the S-SE are separated by an important tectonic lineament. The northern Apennines (NAP) are mainly composed of siliciclastic rocks, and subordinately of chaotic and mixed sedimentary rocks, while the central Apennines (CAP) mainly consist of carbonate rocks. Intermediate percentages of carbonate rocks, mixed and chaotic sedimentary rocks, and siliciclastic deposits are found in the North Internal Apennines (NIAP), in the Southern Apennines (SEAP) and in the Western Sicily (WS). In WS significant percentages of evaporites are also recorded. In the Central and South Eastern Apennines (CEAP and SEAP), high percentages of unconsolidated and consolidated clastic rocks are present, while carbonate rocks dominate the lithology of the Gargano and the Murge Foreland (GF and MF). The similarity between the most represented lithological classes in the Calabro-Peloritano Arc (CPA) and Sardinian Block (SB) is evident, although schistose rocks prevail in CPA while intrusive rocks prevail in SB. Volcanic rocks are extensively represented in the Central and Southern Magmatic Province (CMP and SMP), in the Eastern Sicily (ES), in the Sardinian Block (SB), and subordinately in the Eastern Alps (EAL).

Significant regional differences in the representation of lithologies also exist (Figure 6d). In the original geological dataset, the number of polygons per squared kilometres (black points in Figure 6d) used to represent the lithological variability is strongly heterogeneous across Italy, and is proportional to the geo-lithological complexity of each physiographic region. For instance, the Alpine regions (EAL, CAL, WA), which are characterized by a complex geological architecture and by a very high lithological variability, display the higher polygon density, with values between 1.7 e 2.4 polygons/km$^2$. On the other hand, the Po Plain (PP) records the lowest polygons density, with 0,2 polygons per square kilometre, being characterized by a quite monotonous surface geology, almost totally represented by alluvial deposits. Accordingly, in the Apennine regions, which are (in general) geologically less complex than the Alpine regions, the average polygon density is just over 1 (NAP, NIAP, CAP, SMP, SAP) with a maximum of 1,7 in the Central Magmatic Province (CMP) and a minimum of 0,3 in the south-eastern regions of the foredeep (SEAP) and foreland (MF) domains.

The reclassification of the original geological dataset in the LMI classes determined the merging of adjacent polygons exposing rock unit included in the same lithological class. The process resulted in a drop of the number of polygons in each physiographic region, passing from the original data set to the LMI, which is indicated by the length of the black arrows in Figure 6d. Importantly, the reduction of the number of polygons does not change the relative regional variability of the polygon density.

This means that the simplification introduced by our reclassification does not impact the regional difference in the representation of the lithology.

In Figure 6d, the indicator of polygon density (in black) is flanked by an analogue indicator (in blue) displaying the count of the unique descriptions used within each physiographic region, both in the original data set (blue points) and in the reclassified LMI (blue arrow tips). The number of unique descriptions is generally proportional to the polygon density, but cases of exceptionally high number of unique descriptions (e.g. PP, NAP, NIAP, SAP) are common. Primarily, this is the effect of individual geologists or working groups using several local names to define the same rock unit, thus increasing the number of unique descriptions.

Finally, Figure 6d shows that regional differences in the representation of lithologies may be also related to the different years of publication of the geological sheets encompassed in each region. Figure 6d shows that: i) the geological sheets encompassed in the Alpine region have been surveyed in the 1901-1940 (EAL, WAL) and 1961-1989 (CAL) time intervals; ii) almost all the geological sheets encompassed in the regions of the Italian Peninsula (PP, NAP, NIAP, CEAP, CAP, CMP, SMP, SAP, SEAP, GF, MF) have been surveyed in the 1961-1989 time interval, as those of the Sardinian Block (SB); iii) the geological sheets of Western Sicily (WS) Eastern Sicily (ES) and Calabro Peloritano Arc (CPA) have been surveyed in the 1884-1900 time interval. While it is not clear whether the publication year of the geological sheets plays or not a role in controlling the polygon density in the Alpine regions, the impact of the different years of publications in the representation of the regional lithological variability is dramatic comparing CPA and SB. In fact, despite a similar lithological composition (Figure 6c) and a pre-Alpine common geological history (Alvarez and Shimabukuro, 2009), CPA and SB are characterized by a very different density of polygons (0,3 polygons/km2 for CPA, and 1,3 for SB), due to strong differences in drafting geological sheets published almost 100 years apart from each other.

## 5 Discussions

The main challenge in developing a categorized lithological map lies in balancing accuracy and complexity and still properly representing the diversity of lithological variables using a limited yet reasonable number of classes, to ensure ready interpretation and applicability of the map. We maintain that the 19 classes defined here allow to optimize the use of the map for several applications, with a focus on landslides modelling. Despite the specific goals of this work, we applied a classification that can be reconciled with the ones adopted in global lithological databases (Table 1; Hartmann et al., 2012; Geological Survey of Canada, 1995), emphasizing the dominant rock types. Furthermore, information on the physical characteristics of the dominant rock types available in the original geological legend were used to define specific lithological classes.

For example, metamorphic rocks were split into two broad classes considering the dominant presence of schistose or not schistose rocks, hence according to expected - or not expected - pervasive planar anisotropies within the rock bodies. Similarly, the classes of consolidated and unconsolidated clastic sediments, in our map, consist of two separate classes, according to their expected different geotechnical behaviour. In both cases, differences in physical features (*e.g.* schistose/non-schistose, consolidated/unconsolidated) may impact landslide susceptibility of genetically similar rocks (Bucci et al., 2016b), hence justifying the need of these lithological classes for our scope.

We also included the class Marlstone, quite unusual for generalized lithological characterization at national scale. The need for this class arises from the systematic occurrence of significant marls interbeds within carbonate or siliciclastic rocks, whose representation highlights the cartographic detail of the map. Moreover, it is widely recognized that marls intercalations represent important geo-hydrological and mechanical discontinuities within rocks bodies (e.g. see Peacock et al., 2017), often promoting landslide phenomena (Guzzetti et al., 1996), which is a relevant issue for our purpose. Since our map is designed to be used for landslides studies and modelling, we also decided to maintain the class "landslides", although it covers only 0,1% of the Italian territory. We are aware that this percentage value is strongly underestimated. The Inventory of Italian Landslides (Trigila et al., 2010), still incomplete, counts over 620,000 landslides covering a total area equal to 7.9% of the Italian territory, and occurrence of the different types of landslides gives rise to very different patterns of landslide susceptibility, consistently with the diverse lithological formations (Lombardo et al., 2021). However, we acknowledge that the large difference in percentage values stems from the fact that many efforts in landslide mapping have been made in recent decades, when the 277 sheets of the geological map of Italy at 1: 100,000 scale were already published.

Despite the usage of very specific lithological classes helps a reliable classification of the rock types, the map is still subject to uncertainty considering rock properties of some broad lithological classes. This is highlighted, for instance, by the considerable amount of mixed limestone, marls and shale sediments (5%), including the Chaotic (2.2%) and the Mixed sedimentary (2.8%) classes. Despite carbonate rocks and siliciclastic rocks behave differently for a large range of physical or chemical properties (*e.g.*, weathering processes, dissolution rates or aquifer characteristics), they occur often "mixed" in these two geo-lithological classes, further undistinguishable at the scale of the used maps here.

An additional source of uncertainty remains at the boundaries of the geological sheets, where only discontinuities between contiguous sheets longer than 1 km were resolved, with the exception of 58 segments over the entire national territory. Table 5 represents a contiguity matrix for these 58 segments. Table 5 reveals that 19 segments, 33% of the total, bound polygons pertaining to the Al (Alluvial and marine deposits) class, which is the most represented lithological class at national scale, covering the 25% of the entire national territory. The segments that bound lithological classes belonging to the same genetic groups (metamorphic, magmatic, sedimentary) are 24, 10 of which separate lithological classes of the sedimentary substratum from others belonging to sedimentary covers. Only 15 segments bound lithological classes belonging to different genetic groups. Despite all these segments represent identical inconsistencies from a graphical point of view, their potential negative local effects on the map reliability may be different from a lithological point of view. For instance, for landslide studies, we can consider negligible the potential negative effects of unrealistic, linear lithological boundaries of polygons pertaining to the Al class since they cover (almost) only flat areas of fluvial, alluvial and coastal plain, where landslides are unexpected.

| I level classification → | | *Metamorphic* | | *Magmatic* | | | *Sedimentary* | | | | | | | | | | | | | |
|---|---|---|---|---|---|---|---|---|---|---|---|---|---|---|---|---|---|---|---|---|
| **II level classification →** | | *Metamorphic* | | *Intrusion* | *Cover* | | *Substratum* | | | | | *Undifferentiated Cover* | | | | | | | *Alluvial/Marine* | |
| **III level classification →** | | **Sr** | **Nsr** | **Ir** | **Pr** | **Lb** | **Cr** | **M** | **SM** | **Cm** | **Ssr** | **E** | **Ucr** | **Ccr** | **Gd** | **Mw** | **Ad** | **Li** | **B** | **Al** |
| *Metamorphic* | **Sr** | 0 | 3 | 2 | 0 | 0 | 2 | 0 | 0 | 0 | 1 | 0 | 3 | 1 | 2 | 0 | 0 | 0 | 0 | 1 |
| | **Nsr** | 3 | 0 | 1 | 0 | 0 | 0 | 0 | 0 | 0 | 0 | 0 | 0 | 0 | 1 | 0 | 0 | 0 | 0 | 2 |
| *Magmatic* | **Ir** | 2 | 1 | 0 | 1 | 0 | 0 | 0 | 0 | 0 | 0 | 0 | 0 | 0 | 0 | 0 | 0 | 0 | 0 | 4 |
| | **Pr** | 0 | 0 | 1 | 0 | 0 | 0 | 0 | 0 | 0 | 0 | 0 | 1 | 0 | 1 | 0 | 0 | 0 | 0 | 1 |
| | **Lb** | 0 | 0 | 0 | 0 | 0 | 0 | 0 | 0 | 0 | 0 | 0 | 0 | 0 | 0 | 0 | 0 | 0 | 0 | 0 |
| *Sedimentary substratum* | **Cr** | 2 | 0 | 0 | 0 | 0 | 0 | 1 | 0 | 0 | 2 | 0 | 3 | 2 | 0 | 0 | 0 | 0 | 0 | 1 |
| | **M** | 0 | 0 | 0 | 0 | 0 | 1 | 0 | 0 | 0 | 3 | 0 | 0 | 0 | 0 | 0 | 0 | 0 | 0 | 1 |
| | **SM** | 0 | 0 | 0 | 0 | 0 | 0 | 0 | 0 | 0 | 0 | 0 | 1 | 0 | 0 | 0 | 0 | 0 | 0 | 0 |
| | **Cm** | 0 | 0 | 0 | 0 | 0 | 0 | 0 | 0 | 0 | 1 | 0 | 0 | 0 | 0 | 0 | 0 | 0 | 0 | 1 |
| | **Ssr** | 1 | 0 | 0 | 0 | 0 | 2 | 3 | 0 | 1 | 0 | 0 | 2 | 2 | 0 | 0 | 0 | 0 | 0 | 2 |
| *Undifferentiated sedimentary cover* | **E** | 0 | 0 | 0 | 0 | 0 | 0 | 0 | 0 | 0 | 0 | 0 | 0 | 0 | 0 | 0 | 0 | 0 | 0 | 1 |
| | **Ucr** | 3 | 0 | 0 | 1 | 0 | 3 | 0 | 1 | 0 | 2 | 0 | 0 | 3 | 0 | 0 | 0 | 0 | 0 | 0 |
| | **Ccr** | 1 | 0 | 0 | 0 | 0 | 2 | 0 | 0 | 0 | 2 | 0 | 3 | 0 | 0 | 0 | 0 | 0 | 0 | 2 |
| | **Gd** | 2 | 1 | 0 | 1 | 0 | 0 | 0 | 0 | 0 | 0 | 0 | 0 | 0 | 0 | 0 | 0 | 0 | 0 | 2 |
| | **Mw** | 0 | 0 | 0 | 0 | 0 | 0 | 0 | 0 | 0 | 0 | 0 | 0 | 0 | 0 | 0 | 0 | 0 | 0 | 0 |
| | **Ad** | 0 | 0 | 0 | 0 | 0 | 0 | 0 | 0 | 0 | 0 | 0 | 0 | 0 | 0 | 0 | 0 | 0 | 0 | 0 |
| | **Li** | 0 | 0 | 0 | 0 | 0 | 0 | 0 | 0 | 0 | 0 | 0 | 0 | 0 | 0 | 0 | 0 | 0 | 0 | 0 |
| *Alluvial/Marine* | **B** | 0 | 0 | 0 | 0 | 0 | 0 | 0 | 0 | 0 | 0 | 0 | 0 | 0 | 0 | 0 | 0 | 0 | 0 | 1 |
| | **Al** | 1 | 2 | 4 | 1 | 0 | 1 | 1 | 0 | 1 | 2 | 1 | 0 | 2 | 2 | 0 | 0 | 0 | 1 | 0 |
| **Total number →** | | **15** | **7** | **8** | **4** | **0** | **11** | **5** | **1** | **2** | **13** | **1** | **13** | **10** | **6** | **0** | **0** | **0** | **1** | **19** |

**Table 5:** Contiguity matrix showing the number of the 58 N-S and E-W oriented straight segments longer than 1000 m which bounds each lithological class.

On the other hand, critical differences remain between rocks pertaining to the same genetic group but characterized by different physical properties (schistose/non schistose metamorphic rocks, consolidated/unconsolidated sedimentary clastic rocks). Overall, we consider as resolved the inhomogeneity problems at the boundaries between adjacent geological sheets for segments equal to or greater than 1000 meters, hence considering the remaining 58 segments longer than 1000 meters listed in Table 1 as acceptable and/or negligible exceptions. Since in cartography the admissible error is traditionally assumed to be 1 mm, we maintain that, only along the boundaries of the geological sheets our map is formally correct at the 1:1,000,000 scale, while elsewhere the cartographic detail remains compatible with the 1:100,000 scale. Pushing harmonization operation into more detail would require altering the original data, which is outside the scope of this work.

The design of the LMI allows for further corrections and inclusion of additional information, (*e.g.*, age information, tectonic history, geotechnical properties, fine-coarse grain size ratio) in future versions, customizable for different usage, with expected reduction of general and/or specific uncertainties. Additional information may be organized into more detailed classification levels, although their compilation will require further efforts to collect data from local geo-lithological literature and site-specific investigations.

Since different purposes impose different generalization strategies, other lithological classifications of the Italian rocks are possible, starting from the same source dataset. For instance, aiming at a seismic soil classification of Italy, Forte et al. (2019)

generalized the lithology of Italy using 20 classes, a number comparable to the 19 classes presented here. In Forte et al. (2019)'s classification, a relevant distinction was based on the identification of geo-lithological complexes as geologic bedrock, versus those representative of cover deposits, being the last category directly related to defined values of $V_S$ (average speed of propagation of shear waves), hence particularly relevant for their purpose. On the other hand, the most recent lithological map of Italy provided by ISPRA as a web service is accompanied by a complex legend, articulated in 48 classes aimed at describe age, genesis and chemical-physical characteristics of rocks, focusing on a comprehensive geological rock characterization, without specific applicative purpose. It is evident that different classifications allow different possible usages of the same original dataset, hence, at the same representation scale, different lithological characterizations can be more or less suitable depending on the intended purpose.

Although the general rock composition of the Italian's surface is remarkably similar between the existing digital lithological maps (Table 1, ID 5) the representation of the rock distribution varies largely between them, and have been greatly improved in the present map, especially across geological sheets. Compared to smaller-scale maps (Compagnoni et al., 1976-1983), the main improvements lays in a better representation of complex geological settings. Moreover, a better lithological harmonization along the borders of the original geological sheets distinguishes our map from other maps at the same scale (Servizio Geologico d'Italia, 2004). Figure 7 shows examples for Sicilia, Campania and Lombardia regions, highlighting the general improvement of the map, regardless of the geographical location, geological and geomorphological settings. However, a direct comparison of the maps is difficult due to the different legends (*e.g.* based on geological processes or lithology, or mixing up processes and lithology).

Early versions of the LMI presented here were already used to validate terrain classification of Italy (Alvioli et al., 2020) and to estimate soil parameters for physically based rockfall modelling along the Italian railway (Alvioli et al., 2021). Such versions of the map included a few of the inconsistencies resolved in this work. We expect that a similar use of the map could be extended to study and model other types of landslides in different lithological settings, both widespread in the landscape and along specific infrastructure networks.

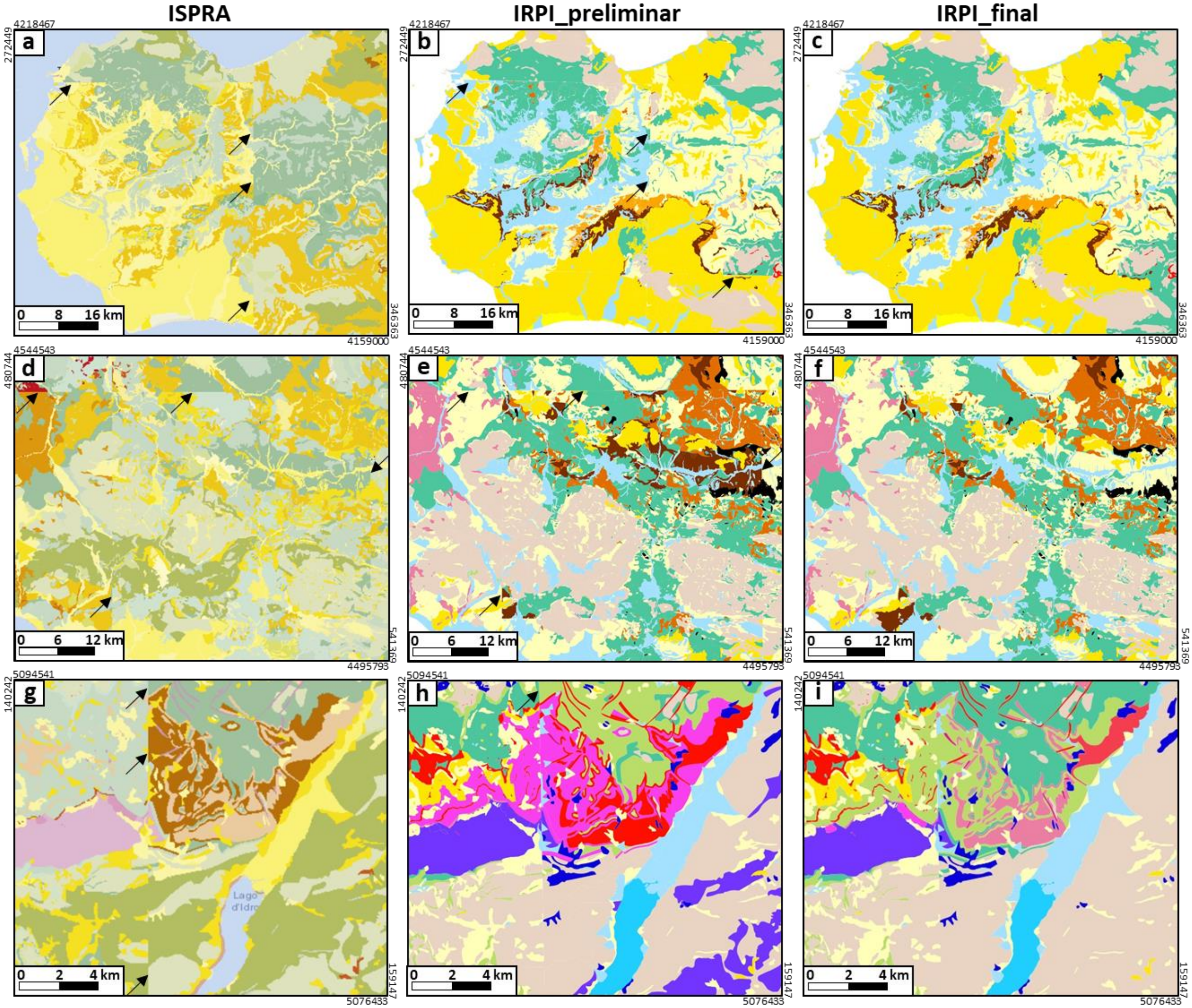


**Figure 7:** Comparison of two different classifications of the same source dataset for selected areas of Sicilia **(a, b, c)**, Campania **(d, e, f)** and Lombardia **(g, h, i)** regions. Examples from the lithological map of Italy according to ISPRA classification as visualized in vector form at the ISPRA website (Table 1, ID 5) are shown in (a), (d) and (g). For the same areas, the lithological map of Italy according to our own preliminar semi-automatic classification partially resolved the major inconsistencies along the boundaries of the geological sheets already present in (a), (d) and (g), even if critical boundaries still remains, see black arrows as reference; Most of the inconsistencies were resolved manually by expert analysis in the final version of our map (c, f, i) leading a substantial improvement of the lithological harmonization along the borders of the original geological sheets.

## 6 Conclusions

This paper described the first freely downloadable lithological map of Italy at the 1:100.000 scale, providing the distribution of rock-attributes and rock-types of the Italian territory in digital format.

The LMI was assembled from 277 sheets of the Geological Map of Italy at the 1: 100,000 scale and distributed in digital vector format through a REST service on the ISPRA website. For the purpose, the rock types associated with the 5.456 unique geological descriptions in the source dataset were identified and translated into the 19 general classes defined here. Adjacent polygons grouped within the same class were dissolved, reducing their number from the original 292,705 to the 180,503 in the final product. Most of the work consisted with database queries, coupled with expert analysis of the location of the polygons using the sheets available at the 1:50,000 scale (where present), and with any potentially useful information sought in regional and local literature. Particular attention was paid to harmonize the lithological information at the boundaries of the original geological sheets. A final technical validation allowed to detect and resolve residual problems, also related to inconsistencies inherited from the source dataset, and guaranteed the overall quality of the work.

The LMI allows the assessment of national scale research questions at high resolution and thus helps to advance our knowledge on the relationships between lithology and surface processes, including multiple geomorphological, geo-hydrological and environmental issues. In addition, the resolution of the LMI highlights the differences in the lithological cover of the different regions and sub-regions, hence facilitating the comparison of results of different regional studies (*e.g.*, susceptibility to landslides and floods).

The map has limits and can be enhanced, in particular in local areas where geo-lithological descriptions in the source dataset were not exhaustive and our knowledge is limited. Inclusion of more detailed regional maps or other relevant additional information, *e.g.*, age, tectonic history, geotechnical properties, fine-coarse grain size ratio are out of the aim of this work, but may be included in future versions. Aware of these and other potential and desirable future upgrades, we provided the LMI with a very simple and open architecture, which allows more details or levels of information to be added and could thus be developed further in accordance with specific scientific questions.

## 7 Data availability

The digital lithological Map of Italy at 1:100.000 is provided in the PANGAEA database. It is publicly available at the following web address: https://doi.org/10.1594/PANGAEA.935673 (Bucci et al. 2022).

## 8 Author contribution

Francesco Bucci (FB), Michele Santangelo (MS), Lorenzo Fongo (LF), Mauro Cardinali (MC) and Ivan Marchesini (IM) decided the classification system, performed multiscale comparative analysis, and drafted the final version of the lithological map. Ivan Marchesini (IM) e Massimiliano Alvioli (MA) prepared the dataset and the script for the final classification. FB, MS, LF, MC, IM and Laura Melelli (LM) compiled the Legend and designed the layout of the final map. FB, MS wrote the text. LF, MC, IM, MA, LM reviewed and integrated the paper at several stages, IM supervised the research activity.

## 9 Competing interests

The authors declare no competing interests.


## 10 Acknowledgements

The work was partly carried out within the FRA.SI (Multi-scale integrated methodologies for seismically-induced landslides risk zonation) project, of the National Research council of Italy (CNR).


## References


Alvarez, W., Shimabukuro D.H.: The geological relationships between Sardinia and Calabria during Alpine and Hercynian times. Italian Journal of Geosciences, 128, 2, 257–268. doi: https://doi.org/10.3301/IJG.2009.128.2.257, 2009.

Alvioli, M., Guzzetti, F., Marchesini, I.: Parameter-free delineation of slope units and terrain subdivision of Italy, Geomorphology, 358, 107-124. https://doi.org/10.1016/j.geomorph.2020.107124, 2020.

Alvioli, M., Marchesini, I., Reichenbach, P., Rossi, M., Ardizzone, F., Fiorucci, F., Guzzetti, F.: Automatic delineation of geomorphological slope units and their optimization for landslide susceptibility modelling, Geosci. Model Dev. 9, 3975–3991. https://doi.org/10.5194/gmd-9-3975-2016, 2016.

Alvioli, M., Santangelo, M., Fiorucci, F., Cardinali, M., Marchesini, I., Reichenbach, P., Rossi, M., Guzzetti, F., Peruccacci, S.: Rockfall susceptibility and network-ranked susceptibility along the Italian railway. Engineering Geology, 2021 (in press).

Amanti, M., Battaglini, L., Campo, V., Cipolloni, C., Congi, M.P., Conte, G., Delogu, D., Ventura, R., Zonetti, C.: The Lithological map of Italy at 1:100.000 scale: An example of re-use of an existing paper geological map. In: 33rd International Geological Conference, IEI02310L - 6-14th August, Oslo (Norway), 2008.

Amanti, M., Battaglini, L., Campo, V., Cipolloni, C., Congi, M.P., Conte, G., Delogu, D., Ventura, R., Zonetti, C.: La carta litologica d'italia alla scala 1:100.000. Atti della 11a Conferenza Nazionale ASITA, Centro Congressi Lingotto, Torino, 6–9 Novembre 2007, http://atti.asita.it/Asita2007/Pdf/119.pdf, 2007.

Amodio Morelli, L., Bonardi, G., Colonna, V., Dietrich, D., Giunta G., Liguori, V., Lorenzoni, S., Paglianico, A., Perrone, V., Piccarreta, G., Russo, M., Scandone, P., Zanettin, E., Zuppetta, A.: L'arco Calabro Peloritano nell'Orogene Appenninico-Magrebide, Memorie della Società Geologica Italiana, 17, 1-60, 1976.

Asch, K.: The 1:5 million international geological map of Europe and adjacent areas. Bundesanstalt fur Geowissenschaften und Rohstoffe, Commission of the Geological Map of the World, Subcommission for Europe. BGR, Hannover, 2005.

Bentivenga, M., Coltorti, M., Prosser, G., Tavarnelli, E.: Deformazioni distensive recenti nell'entroterra del Golfo di Taranto: implicazioni per la realizzazione di un deposito geologico per scorie nucleari nei pressi di Scanzano Jonico (Basilicata), Boll. Soc. Geol. It., 123, 3, 391-404, 2004.

Boni, C.F., Bono, P., Funicello, R., Parotto, M., Praturlon, A., Fanelli, M.: Carta delle manifestazioni termali e dei complessi idrogeologici, scala 1:1.000.000. In: Contributo alla conoscenza delle risorse geotermiche del territorio italiano. CNR, Progetto Finalizzato Energetica, Sottoprogetto Energia Geotermica, Roma, 1984.

Bonomo, R., Capotorti, F., D'Ambrogi, C., Di Stefano, R., Graziano, R., Martarelli, L., Pampaloni, M.L., Pantaloni, M., Ricci, V., Compagnoni, B., Galluzzo, F., Tacchia, D., Masella, G., Pannuti, V., Ventura, R., Vitale, V.: Carta geologica d'Italia alla scala 1:1.250.000, Serv. Geol. d'It., APAT, Roma, 2005.

Bortolotti, V., Fazzuoli, M., Pandelli, E., Principi, G., Babbini, A., Corti, S.: Geology of Central and Eastern Elba Island, Italy, Ofioliti, 26(2): 97-150, 2001.

Brogi, A., Liotta, D.: Fluid flow paths in fossil and active geothermal fields: the Plio-Pleistocene Boccheggiano-Montieri and the Larderello areas, Geological Field Trips of the Italian Geological Society, vol. 3(2.2), ISSN: 2038- 4947, doi:10.3301/GFT.2011.03, 2011.

Brozzetti, F.: Geological map (1: 25.000 scale) of the Northern Umbria Preapennines in the M:S:M: Tiberina area (Umbria Italy). Boll. Soc. Geol. It, 126, 511-529, 2007.

Bucci, F., Novellino, R., Guglielmi, P., Prosser, G., & Tavarnelli, E. (2012). Geological map of the northeastern sector of the high Agri Valley, Southern Apennines (Basilicata, Italy). Journal of Maps, 8, 282–292. https://doi.org/10.1080/17445647.2012.722403

Bucci, F., Novellino, R., Tavarnelli, E., Prosser, G., Guzzetti, F., Cardinali, M., Gueguen, E., Guglielmi, P., Adurno, I.: Frontal collapse during thrust propagation in mountain belts: a case study in the Lucania Apennines, Southern Italy, J. Geol. Soc. 171, 571–581, https://doi.org/10.1144/jgs2013-103, 2014.

Bucci, F., Mirabella, F., Santangelo, M., Cardinali, M., Guzzetti, F.: Photo-geology of the Montefalco Quaternary Basin, Umbria, Central Italy, Journal of Maps 12:314–322, https://doi.org/10.1080/17445647.2016.1210042, 2016a.

Bucci, F., Santangelo, M., Cardinali, M., Fiorucci, F., Guzzetti, F.: Landslide distribution and size in response to Quaternary fault activity: the Peloritani Range, NE Sicily, Italy, Earth Surf. Process. Landf. 41, 711–720, https://doi.org/10.1002/esp.3898, 2016b.

Bucci, F., Tavarnelli, E., Novellino, R., Palladino, G., Guglielmi, P., Laurita, S., Prosser, G., Bentivenga, M.: The History of the Southern Apennines of Italy Preserved in the Geosites Along a Geological Itinerary in the High Agri Valley, Geoheritage 11, 1489–1508, https://doi.org/10.1007/s12371-019-00385-y, 2019.

Bucci, F., Novellino, R., Guglielmi, P., Tavarnelli, E.: Growth and dissection of a fold and thrust belt: the geological record of the High Agri Valley, Italy. J. Maps 16, 245–256, https://doi.org/10.1080/17445647.2020.1737254, 2020.

Bucci, F., Santangelo, M., Fongo, L., Alvioli, M., Cardinali, M., Melelli, L., Marchesini, I.: A new digital lithological Map of Italy at 1:100.000 scale. PANGAEA, https://doi.org/10.1594/PANGAEA.935673 (2022).

Calamita, F., Esestime, P., Paltrinieri, W., Scisciani, V., Tavarnelli, E. (2009). Structural inheritance of pre- and synorogenic normal faults on the arcuate geometry of Pliocene-Quaternary thrusts: Examples from the Central and Southern Apennine Chain. Italian Journal of Geosciences (Boll. Soc. Geol. It.), 128, 2, 381-394 (DOI:10.3301/IJG.2009.128.2.381)

Campobasso, C., Salvati, L., Vita, L. Eds.: Evoluzione dei bacini neogenici e loro rapporti con il magmatismo plio-quaternario dell’area tosco-laziale (Pisa, 1991), Mem. Descr. Carta Geol. d’It., 49, pp. 375, Ser. Geol. d’It., Roma, 1994.

Carmignani, L., Conti, P., Cornamusini, G., Pirro, A.: Geological map of Tuscany (Italy), J. Maps 9, 487–497, https://doi.org/10.1080/17445647.2013.820154, 2013.

Carmignani, L.: Geologia della Sardegna. Note illustrative della Carta Geologica della Sardegna a scala 1:200.000. Mem. Descr. Carta Geol. d’It., 60: pp. 283, Serv. Geol. d’It., Roma, 2001.

Catanzariti, R., Ottria, G., Cerrina Feroni, A.: Carta geologico-strutturale dell’Appennino Emiliano-Romagnolo. Scala 1:250.000. RER - Servizio Geologico, Sismico e dei Suoli; CNR - Istituto di Geoscienze e Georisorse, Pisa, 2002.

Celico, P.B., De Vita, P., Monacelli, G., Scalise, A.R., Tranfaglia, G.: Carta idrogeologica dell’Italia Meridionale, scala 1:250.000. ISPRA, Roma, 2005.

Centamore, E., Panbianchi, G., Deiana, G., Calamita, F., Cello, G., Dramis, F., Gentili, B., Nanni, T.: Ambiente fisico delle Marche. Geologia, Geomorfologia, Idrogeologia alla scala 1:100.000. Regione Marche, 1991.

Centamore, E., Rossi, D., Tavarnelli, E. (2009). Geometry and kinematics of Triassic-to-Recent structures in the Northern-Central Apennines: a review and an original working hypothesis. Italian Journal of Geosciences (Boll. Soc. Geol. It.), 128, 2, 419-432 (DOI: 10.3301/IJG.2009.128.2.419).

Chiarini, E., D’Orefice, M., Graciotti, R.: Le unità stratigrafiche di riferimento nella rappresentazione cartografica dei depositi plio-quaternari continentali nel Progetto CARG. Esempi: Arco alpino, Pianura Padana e Sardegna. Il Quaternario, 21, 1A, 51-56, 2008.

Cipolloni, C., Pantaloni, M., Ventura, R., Vitale, V., Tacchia, D.: The GEO1MDB: the database of the 1:1,000,000 scale geological map of Italy. In: 6th EUREGEO Proceeding, 1: 218-221, 2009.

Compagnoni, B.: La Carta geologica d’Italia, alla scala 1.1.000.000. Mem. Descr. Carta Geol. It., 71, 207-212, 2004.

Compagnoni, B., Damiani, A.V., Valletta, M.: Carta geologica d'Italia alla scala 1:500.000. In 5 fogli e note illustrative, Servizio Geologico d'Italia, Roma, 1976-1983.

Consiglio Nazionale delle Ricerche: Structural model of Italy and gravity map. Quaderni della Ricerca Scientifica, 114, 3, 1990.

Console, F., Pantaloni, M., Petti, F.M., Tacchia, D.: La cartografia del Servizio geologico d'Italia = The Geological survey of Italy mapping, ISBN:978-88-9311-052-5, 2017.

Conti, P., Cornamusini, G., Carmignani, L.: An outline of the geology of the Northern Apennines (Italy), with geological map at 1:250,000 scale, Ital. J. Geosci. 139, 149–194, https://doi.org/10.3301/IJG.2019.25, 2020.

Corpo Reale delle Miniere: Carta mineraria d'Italia. Scala 1:500.000, Roma, 1926-1935.

Coulthard, T.J.: Landscape evolution models: A software review, Hydrol. Processes, 15, 1, 165–173, doi:10.1002/hyp.426, 2001.

D'Ambrogi, C., Scrocca, D., Pantaloni, M., Valeri, V., Doglioni, C.: Exploring Italian geological data in 3D. In: M. BELTRANDO, A. PECCERILLO, M. MATTEI, S. CONTICELLI & C. DOGLIONI: The Geology of Italy. Journal of the Virtual Explorer, 36, paper 33. doi:10.3809/jvirtex.2010.00256, 2010.

De Graaf, I.E.M., Van Beek, R.L.P.H., Gleeson, T., Moosdorf, N., Schmitz, O., Sutanudjaja, E.H., Bierkens, M.F.P.: A global-scale two-layer transient groundwater model: Development and application to groundwater depletion. Adv. Water Resour. 102, 53–67. https://doi.org/10.1016/j.advwatres.2017.01.011, 2017.

De Rita D., Fabbrini, M., Cimarelli, C. (2004) - Evoluzione pleistocenica del margine tirrenico dell'Italia centrale tra eustatismo, vulcanismo e tettonica. Il Quaternario, 17(2): 523-536.

De Sousa, L.M., Poggio, L., Batjes, N.H., Heuvelink, G.B.M., Kempen, B., Riberio, E., Rossiter, D., 2020. SoilGrids 2.0: producing quality-assessed soil information for the globe. SOIL Discuss. 1–37. https://doi.org/10.5194/soil-2020-65

Delogu, D., Campo, V., Cipolloni, C., Congi, M.P., Falcetti, S., Moretti, P. Pampaloni, M. L., Pantaloni, M., Roma, M., Ventura, R.: Il Portale del Servizio Geologico d'Italia: uno strumento al servizio dei geologi professionisti. Professione Geologo, 32, 4, 24-27, 2012.

Donnini, M., Marchesini, I., Zucchini, A., 2020a. Geo-LiM: a new geo-lithological map for Central Europe (Germany, France, Switzerland, Austria, Slovenia, and Northern Italy) as a tool for the estimation of atmospheric CO 2 consumption. J. Maps 16, 43–55. https://doi.org/10.1080/17445647.2019.1692082

Donnini, M., Marchesini, I., Zucchini, A., 2020b. A new Alpine geo-lithological map (Alpine-Geo-LiM) and global carbon cycle implications. GSA Bull. 132, 2004–2022. https://doi.org/10.1130/B35236.1

Dürr, H.H., Meybeck, M., Dürr, S.H., 2005. Lithologic composition of the Earth's continental surfaces derived from a new digital map emphasizing riverine material transfer. Glob. Biogeochem. Cycles 19, n/a-n/a. https://doi.org/10.1029/2005GB002515

Forte, G., Chioccarelli, E., De Falco, M., Cito, P., Santo, A., Iervolino, I., 2019. Seismic soil classification of Italy based on surface geology and shear-wave velocity measurements. Soil Dyn. Earthq. Eng. 122, 79–93. https://doi.org/10.1016/j.soildyn.2019.04.002

Ge.Mi.Na. (1962). Ligniti e torbe dell'Italia continentale. Geomineraria nazionale, 1–319

Geological Survey of Canada, Open File 2915d, doi:10.4095/195142, 1995, https://mrdata.usgs.gov/geology/world/map-us.html#home (access date 2021/05/07)

Giannandrea, P., La Volpe, L., Principe, C., Schiattarella, M. (2006) - Carta geologica del Monte Vulture. Scala 1:25.000. In: PRINCIPE C., La geologia del Monte Vulture, CNR, Regione Basilicata. pp. 217.

Giardino, M. & Fioraso, G. (1998) - Cartografia geologica delle formazioni superficiali in aree di catena montuosa: il rilevamento del F. “Bardonecchia” nell’ambito del progetto CARG. Mem. Sci. Geol., 50: 133-153

Gibbs, M.T., Kump, L.R., 1994. Global chemical erosion during the Last Glacial Maximum and the present: Sensitivity to changes in lithology and hydrology. Paleoceanography 9, 529–543. https://doi.org/10.1029/94PA01009

Girotti, O. & Mancini, M. (2003) - Plio-Pleistocene stratigraphy and relations between marine and non-marine successions in the middle valley of the Tiber river (Latium, Umbria). Il Quaternario, Italian Journal of Quaternary Sciences, 16 (1 bis): 89-106.

Giustini, F., Ciotoli, G., Rinaldini, A., Ruggiero, L., Voltaggio, M.: Mapping the geogenic radon potential and radon risk by using Empirical Bayesian Kriging regression: A case study from a volcanic area of central Italy, Science of The Total Environment, 661, 449-464, https://doi.org/10.1016/j.scitotenv.2019.01.146, 2019.

Gleeson, T., Smith, L., Moosdorf, N., Hartmann, J., Dürr, H. H., Manning, A. H., van Beek, L. P. H., and Jellinek, A. M. (2011), Mapping permeability over the surface of the Earth, Geophys. Res. Lett., 38, L02401, doi:10.1029/2010GL045565.

Gueguen, E., Tavarnelli, E., Renda, P., Tramutoli, M. (2010). The southern Tyrrhenian Sea margin: an example of lithospheric scale strike-slip duplex. Italian Journal of Geosciences (Boll. Soc. Geol. It.), 129, 3, 496-505 (DOI: 10.3301/IJG.2010.15).

Guzzetti, F., Cardinali, M., Reichenbach, P. (1996). The influence of structural setting and lithology on landslide type and pattern. Environmental and Engineering Geosciences, 2, 531–555. doi:10.2113/gseegeosci.ii.4.531

Han, L., Fuqiang, L., Zheng, D., Weixu, X. (2018). A lithology identification method for continental shale oil reservoir based on BP neural network. Journal of Geophysics and Engineering, 15(3), 895–908. https://doi.org/10.1088/1742-2140/aaa4db

Hartmann, J., N. Jansen, H. H. Dürr, A. Harashima, K. Okubo, and S. Kempe (2010), Predicting riverine dissolved silica fluxes to coastal zones from a hyperactive region and analysis of their first order controls, Int. J. Earth Sci., 99 (1), 207–230, doi:10.1007/s00531-008-0381-5

Hartmann, J., Dürr, H.H., Moosdorf, N., Meybeck, M., Kempe, S., 2012. The geochemical composition of the terrestrial surface (without soils) and comparison with the upper continental crust. Int. J. Earth Sci. 101, 365–376. https://doi.org/10.1007/s00531-010-0635-x

Hartmann, J., Moosdorf, N., 2012. The new global lithological map database GLiM: A representation of rock properties at the Earth surface: TECHNICAL BRIEF. Geochem. Geophys. Geosystems 13. https://doi.org/10.1029/2012GC004370

Horton, J.D., 2017, The State Geologic Map Compilation (SGMC) geodatabase of the conterminous United States (ver. 1.1, August 2017): U.S. Geological Survey data release, https://doi.org/10.5066/F7WH2N65.

Ispra & Parco Nazionale del Cilento, Vallo di Diano e Alburni (2013) - Carta geologica con elementi tematici e carta dei paesaggi sottomarini del Parco Nazionale del Cilento, Vallo di Diano e Alburni (European and Global Geopark). Salerno. http://www.isprambiente.gov.it/it/progetti/suolo-eterritorio-1/carta-geologica-del-parco-del-cilento-vallo-di-diano-e-degli-alburni

Lentini, F. & Carbone, S. Eds. (2014) - Geologia della Sicilia. Mem. Descr. Carta Geol. d'It., 95: pp. 413, Serv. Geol. d'It., Roma

Lombardo, L., Loche, M., Marchesini, I., Alvioli, M., Bakka, H. (2021). A strategy to obtain statistically significant landslide susceptibility maps from a spatially unbalanced, nation-wide inventory in Italy. Submitted for publication.

Lorenzo-Lacruz, J., Garcia, C., Morán-Tejeda, E., 2017. Groundwater level responses to precipitation variability in Mediterranean insular aquifers. J. Hydrol. 552, 516–531. https://doi.org/10.1016/j.jhydrol.2017.07.011

Marchesini, I., Cencetti, C., & De Rosa, P., 2009. A preliminary method for the evaluation of the landslides volume at a regional scale. GeoInformatica, 13(3), 277–289. https://doi.org/10.1007/s10707-008-0060-5

Marchesini, I., Mergili, M., Rossi, M., Santangelo, M., Cardinali, M., Ardizzone, F., Fiorucci, F., Schneider-Muntau, B., Fellin, W., & Guzzetti, F., 2014. A GIS Approach to Analysis of Deep-Seated Slope Stability in Complex Geology. In K. Sassa, P. Canuti, & Y. Yin (Eds.), Landslide Science for a Safer Geoenvironment (pp. 483–489). Springer International Publishing. https://doi.org/10.1007/978-3-319-05050-8_75

Mergili, M., Marchesini, I., Rossi, M., Guzzetti, F., & Fellin, W., 2014a. Spatially distributed three-dimensional slope stability modelling in a raster GIS. Geomorphology, 206, 178–195. https://doi.org/10.1016/j.geomorph.2013.10.008

Mergili, M., Marchesini, I., Alvioli, M., Metz, M., Schneider-Muntau, B., Rossi, M., Guzzetti, F., 2014b. A strategy for GIS-based 3-D slope stability modelling over large areas. Geosci. Model Dev. 7, 2969–2982. https://doi.org/10.5194/gmd-7-2969-2014

Ministero dei Lavori Pubblici, Ufficio Idrografico, Sezione Geologica (1948) - Carta Geologica d'Italia alla scala 1:100.000 – F. 35 Riva. Firenze.

Mirabella, F., Bucci, F., Santangelo, M., Cardinali, M., Caielli, G., De Franco, R., Guzzetti, F., & Barchi, M. R. (2018). Alluvial fan shifts and stream captures driven by extensional tectonics in central Italy. Journal of the Geological Society, 175, 788–805. https://doi.org/10.1144/jgs2017-138.

Mori, F., Mendicelli, A., Moscatelli, M., Romagnoli, G., Peronace, E., Naso, G., 2020. A new Vs30 map for Italy based on the seismic microzonation dataset. Eng. Geol. 275, 105745. https://doi.org/10.1016/j.enggeo.2020.105745

Novellino, R., Bucci, F., Tavarnelli, E., 2021. Structural investigation of background features and normal faults affecting the Calcari con Selce Formation, Southern Apennines, Italy. Ital. J. Geosci. 140, 1–21. https://doi.org/10.3301/ijg.2020.31

Onegeology: http://www.onegeology.org/portal/home.html (access date 2021/05/07)

Pantaloni, M. (2011) - La Carta geologica d'Italia alla scala 1:1.000.000: una pietra miliare nel percorso della conoscenza geologica. Geologia Tecnica & Ambientale, 2-3(11): 88-99

Patacca, E., Scandone, P., Bellatalla, M., Perilli, N., Santini, U. (1991) - La zona di giunzione tra l'arco Appennino settentrionale e l'arco Appennino meridionale nell'Abruzzo e nel Molise. Studi Geol. Camerti, Vol. Spec. 2: 417-441.

Peacock, D.C.P., Anderson, M.W., Rotevatn, A., Sanderson, D.J., Tavarnelli, E. (2017). The interdisciplinary use of "overpressure". Journal of Volcanology and Geothermal Research, 341, 1-5.

Piana, F., Fioraso, G., Irace, A., Mosca, P., d'Atri, A., Barale, L., Falletti, P., Monegato, G., Morelli, M., Tallone, S., Vigna, G.B., 2017. Geology of Piemonte region (NW Italy, Alps–Apennines interference zone). J. Maps 13, 395–405. https://doi.org/10.1080/17445647.2017.1316218

Prosser, G. (2000) The development of the North Giudicarie fault zone (Insubric line, Northern Italy). Journal of Geodynamics, 30, 1-2, 229-250

R. Ufficio Geologico (1884a) - Carta Geologica d'Italia alla scala 1:100.000 – F. 248 Trapani. Roma.

R. Ufficio Geologico (1884b) - Carta Geologica d'Italia alla scala 1:100.000 – F. 249 Palermo. Roma.

R. Ufficio Geologico (1884c) - Carta Geologica d'Italia alla scala 1:100.000 – F. 257 Castevetrano. Roma.

R. Ufficio Geologico (1884d) - Carta Geologica d'Italia alla scala 1:100.000 – F. 258 Corleone. Roma.

R. Ufficio Geologico (1884e) - Carta Geologica d'Italia alla scala 1:100.000 – F. 266 Sciacca. Roma.

R. Ufficio Geologico (1900) - Carta Geologica d'Italia alla scala 1:100.000 – F. 228 Cetraro. Roma.

Raia, S., Alvioli, M., Rossi, M., Baum, R.L., Godt, J.W., Guzzetti, F., 2014. Improving predictive power of physically based rainfall-induced shallow landslide models: a probabilistic approach. Geosci. Model Dev. 7, 495–514. https://doi.org/10.5194/gmd-7-495-2014

Reichenbach, P., Rossi, M., Malamud, B.D., Mihir, M., Guzzetti, F., 2018. A review of statistically-based landslide susceptibility models. Earth-Sci. Rev. 180, 60–91. https://doi.org/10.1016/j.earscirev.2018.03.001

Roche, V., Bouchot, V., Beccaletto, L., Jolivet, L., Guillou-Frottier, L., Tuduri, J., Bozkurt, E., Oguz, K., Tokay, B., 2019. Structural, lithological, and geodynamic controls on geothermal activity in the Menderes geothermal Province (Western Anatolia, Turkey). Int. J. Earth Sci. 108, 301–328. https://doi.org/10.1007/s00531-018-1655-1

Ronchi, A., Cassinis, G., Durand, M., Fontana, D., Oggiano, G., Stefani, C., 2011. Stratigrafia e analisi di facies della successione continentale permiana e triassica della Nurra: confronti con la Provenza e ricostruzione paleogeografica. Geol. Field Trips 3, 1–43. https://doi.org/10.3301/GFT.2011.01

Rossi, M., Reichenbach, P., 2016. LAND-SE: a software for statistically based landslide susceptibility zonation, version 1.0. Geosci. Model Dev. 9, 3533–3543. https://doi.org/10.5194/gmd-9-3533-2016

Sarro, R., Mateos, R. M., Reichenbach, P., Aguilera, H., Riquelme, A., Hernández-Gutiérrez, L. E., Martín, A., Barra, A., Solari, L., Monserrat, O., Alvioli, M., Fernández-Merodo, J. A., López-Vinielles, J., Herrera, G. (2021). Geotechnics for rockfall assessment in the volcanic island of Gran Canaria (Canary Islands, Spain). Journal of Maps 16(2), 605-613 (2020).

Santangelo, M., Gioia, D., Cardinali, M., Guzzetti, F., & Schiattarella, M. (2013). Interplay between mass movement and fluvial network organization: An example from southern Apennines. Italy Geomorphology, 188, 54–67.

Schiattarella, M., Beneduce, P., Di Leo P., Giano, S.I., Giannandrea, P., Principe, C. (2005) - Assetto strutturale ed evoluzione morfotettonica quaternaria del vulcano del Monte Vulture (Appennino lucano). Boll. Soc. Geol. It., 124: 543-562.

Schlögel, R., Marchesini, I., Alvioli, M., Reichenbach, P., Rossi, M., Malet, J.-P., 2018. Optimizing landslide susceptibility zonation: Effects of DEM spatial resolution and slope unit delineation on logistic regression models. Geomorphology 301, 10–20. https://doi.org/10.1016/j.geomorph.2017.10.018

Servizio Geologico d'Italia (1970a) - Carta Geologica d'Italia alla scala 1:100.000 – F. 34 Breno. E.I.R.A., Firenze

Servizio Geologico d'Italia (1970b) - Carta Geologica d'Italia alla scala 1:100.000 – F. 186 S. Angelo dei Lombardi. Ercolano (Napoli)

Servizio Geologico d'Italia (1968a) - Carta Geologica d'Italia alla scala 1:100.000 – F. 36 Schio. Bergamo.

Servizio Geologico d'Italia (1965) - Carta Geologica d'Italia alla scala 1:100.000 – F. 185 Salerno. E.I.R.A., Firenze

Servizio Geologico d'Italia (1969) - Carta Geologica d'Italia alla scala 1:100.000 – F. 199 Potenza. Roma.

Servizio Geologico d'Italia (1964) - Carta Geologica d'Italia alla scala 1:100.000 – F. 163 Lucera. E.I.R.A., Firenze.

Servizio Geologico d'Italia (1955) - Carta Geologica d'Italia alla scala 1:100.000 – F. 265 Mazzara del Vallo. Firenze.

Servizio Geologico d'Italia (1970c) - Carta Geologica d'Italia alla scala 1:100.000 – F. 220 Verbicaro. Ercolano (Napoli)

Servizio Geologico d'Italia (1968b) - Carta Geologica d'Italia alla scala 1:100.000. F. 122 Perugia. Bergamo.

Servizio Geologico d'Italia (1970d) - Carta Geologica d'Italia alla scala 1:100.000 - F. 198 Eboli. Roma.

Servizio Geologico d'Italia (1970e) - Carta Geologica d'Italia alla scala 1:100.000 – F. 187 Melfi. Ercolano (Napoli).

Servizio Geologico d’Italia (2004) - Carta geologica d’Italia interattiva. Interactive geological map of Italy: 1:100.000. 3 CD. M. AMANTI, R. BONTEMPO, P. CARA (a cura di). 1a edizione, Realizzato da Etruria innovazione.

Servizio Geologico d’Italia (1972) - Carta Geologica d’Italia alla scala 1:50.000, F. 027 Bolzano, Firenze.

Servizio Geologico d’Italia (1977) - Carta Geologica d’Italia alla scala 1:50.000, F. 028 La Marmolada, Firenze.

Servizio Geologico d’Italia (2002) - Carta Geologica d’Italia in scala 1:50.00, F. 132-152-153, Bardonecchia.

Servizio Geologico d’Italia (2005a) - Carta Geologica d’Italia alla scala 1:50.000, F. 503 Vallo della Lucania. APAT, Roma.

Servizio Geologico d’Italia (2005b) - Carta geologica d’Italia alla scala 1:50.000, F. 256 Rimini. APAT, Roma.

Servizio Geologico d’Italia (2005c) - Carta Geologica d’Italia alla scala 1:1.250.000. APAT, S.EL.CA., Firenze.

Servizio Geologico d’Italia (2005d) - Carta Geologica d’Italia alla scala 1:50.000, F. 215 Bedonia. APAT, Roma.

Servizio Geologico d’Italia (2006) - Carta Geologica d’Italia alla scala 1:50.000, F. 214 Bargagli. APAT, Roma.

Servizio Geologico d’Italia (2008) - Carta Geologica d’Italia alla scala 1:50.000, F. 058 Monte Adamello. APAT, Roma.

Servizio Geologico d’Italia (2009) - Carta Geologica d’Italia alla scala 1:50.000, F. 031 Ampezzo. ISPRA, Roma.

Servizio Geologico d’Italia (2009) - Carta Geologica d’Italia alla scala 1:50.000, F. 599 Patti. ISPRA, Roma.

Servizio Geologico d’Italia (2010) - Carta Geologica d’Italia alla scala 1:50.000, F. 258-271 San Remo. ISPRA, Roma.

Servizio Geologico d’Italia (2010) - Carta Geologica d’Italia alla scala 1: 50.000, F. 504 Sala Consilina. ISPRA, Roma.

Servizio Geologico d’Italia (2010) - Carta Geologica d’Italia alla scala 1:50.000, F. 228 Cairo Montenotte. ISPRA, Roma.

Servizio Geologico d’Italia (2011) - Carta Geologica d’Italia alla scala 1:50.000, F. 99 Iseo. ISPRA, Roma.

Servizio Geologico d’Italia (2011) - Carta Geologica d’Italia alla scala 1:50.000, F. 089 Courmayeur. ISPRA, Roma.

Servizio Geologico d’Italia (2011) - Carta Geologica d’Italia alla scala 1:50.000, F. 587-600 Milazzo-Barcellona P. di G., S.EL.CA., Firenze.

Servizio Geologico d’Italia (2011) - Carta Geologica d’Italia alla scala 1:1.000.000. ISPRA, Roma.

Servizio Geologico d’Italia (2012) - Carta Geologica d’Italia alla scala 1:50.000, F. 564 Carbonia. ISPRA, Roma.

Servizio Geologico d’Italia (2012) - Carta Geologica d’Italia alla scala 1:50.000, F. 098 Bergamo. ISPRA, Roma.

Servizio Geologico d’Italia (2012) - Carta Geologica d’Italia alla scala 1: 50.000, F. 489 Marsico Nuovo. ISPRA, Roma.

Servizio Geologico d’Italia (2014) - Carta Geologica d’Italia alla scala 1: 50.000, F. 505 Moliterno. ISPRA, Roma.

Servizio Geologico d’Italia (2015) - Carta Geologica d’Italia alla scala 1:50.000, F. 555 Iglesias. ISPRA, Roma.

Servizio Geologico d’Italia (2015) - Carta Geologica d’Italia alla scala 1: 50.000, F. 580 Soverato. ISPRA, Roma.

Servizio Geologico d’Italia (2015) - Carta Geologica d’Italia alla scala 1:50.000, F. 070 Monte Cervino. ISPRA, Roma.

Servizio Geologico d’Italia (2016) - Carta Geologica d'Italia alla scala 1:50.000, F. 280 Fossombrone. ISPRA, Roma.

Tavarnelli E. (1997). Structural evolution of a foreland fold-and-thrust belt: the Umbria-Marche Apennines, Italy. Journal of Structural Geology, 19, 523-534

Tavarnelli, E., Renda, P., Pasqui, V., Tramutoli, M. (2003a). The effects of post-orogenic extension on different scales: an example from the Apennine–Maghrebide fold-and-thrust belt, SW Sicily. Terra Nova, 15, 1-7, 2003.

Tavarnelli, E., Renda, P., Pasqui, V., Tramutoli, M. (2003b). Composite structures resulting from negative inversion: an example from the Isle of Favignana (Egadi Islands). Bollettino della Società Geologica Italiana, 122, 319-325.

Trigila, A., Iadanza, C., & Spizzichino, D. (2010). Quality assessment of the Italian landslide inventory using GIS processing. Landslides, 7(4), 455–470. https://doi.org/10.1007/s10346-010-0213-0

UNESCO-IUGS (2016) – International Stratigraphic chart (versione aggiornata reperibile nel sito: http://www.stratigraphy.org/index.php/ics-chart-timescale)

Vanmaercke, M., Panagos, P., Vanwalleghem, T., Hayas, A., Foerster, S., Borrelli, P., Rossi, M., Torri, D., Casali, J., Borselli, L., Vigiak, O., Maerker, M., Haregeweyn, N., De Geeter, S., Zgłobicki, W., Bielders, C., Cerdà, A., Conoscenti, C., de Figueiredo, T., Evans, B., Golosov, V., Ionita, I., Karydas, C., Kertész, A., Krása, J., Le Bouteiller, C., Radoane, M., Ristić, R., Rousseva, S., Stankoviansky, M., Stolte, J., Stolz, C., Bartley, R., Wilkinson, S., Jarihani, B., Poesen, J. (2021). Measuring, modelling and managing gully erosion at large scales: A state of the art. Earth-Sci. Rev. 103637. https://doi.org/10.1016/j.earscirev.2021.103637

Vezzani, L., Festa, A., Ghisetti, F.C., 2010. Geology and tectonic evolution of the central-southern Apennines, Italy, Special paper. Geological Society of America, Boulder, Colo.

Vignaroli, G., Mancini, M., Bucci, F., Cardinali, M., Cavinato, G. P., Moscatelli, M., Putignano, M. L., Sirianni, P., Santangelo, M., Ardizzone, F., Cosentino, G., Di Salvo, C., Fiorucci, F., Gaudiosi, I., Giallini, S., Messina, P., Peronace, E., Polpetta, F., Reichenbach, P.,…Stigliano, F. (2019). Geology of the central part of the Amatrice Basin (Central Apennines, Italy). Journal of Maps, 15(2), 193–202. https://doi: 10.1080/17445647.2019.1570877.

Vojtek, M., Vojteková, J. 2019.: Flood Susceptibility Mapping on a National Scale in Slovakia Using the Analytical Hierarchy Process. Water 2019, 11, 364. https://doi.org/10.3390/w11020364

## APPENDIX

### Data acquisition procedure

ISPRA exhibits a REST service for the publication of spatial data (Table 1, ID 9). The acronym REST stands for "REpresentational State Transfer", which is an architectural style to develop services using the http data transfer protocol. In particular, ISPRA uses the ArcGIS REST API, the Advanced Programming Interface REST developed by ESRI through the proprietary ArcGIS Online platform. The ESRI API can be queried through specific http requests (for example of GET type, in which the service address is followed by a series of key-value information) that allow, for example, to obtain the representation in JSON (JavaScript Object Notation) format of geometries (geospatial layer features) and associated attributes. Normally this service is limited to the return of a maximum number of features for each request. The acquisition of the database required (i) knowledge of the REST service APIs and (ii) a procedure for the automatic download of subsets of data, which cannot be downloaded in a single piece by design of the website, and (iii) merging of all of the subsets into a single vector map. To execute the download, we prepared a script to download subsets of 100 polygons (geometric features) for each single call to the service, using the Linux *wget* command. The procedure is simple, and consists of a loop in which, at each iteration, a number ($\Delta$) of polygons (100, in the actual case), out of the 300,000 total available polygons. Given that the API of the REST service database was unknown to us, we followed a trial-and error procedure to obtain a working script. Downloaded data consisted of 2,927 files in GeoJSON format, which we converted to a single ESRI Shapefile using the GDAL/OGR library.